12-2003

New Vibroseis data and interpretations from the Shebsh oil and gas field, southwestern Russia

Charles Joel Luckow

To the Graduate Council:

I am submitting herewith a thesis written by Charles Joel Luckow entitled "New Vibroseis data and interpretations from the Shebsh oil and gas field, southwestern Russia." I have examined the final electronic copy of this thesis for form and content and recommend that it be accepted in partial fulfillment of the requirements for the degree of Master of Science, with a major in Geology.

Richard T. Williams, Major Professor

We have read this thesis and recommend its acceptance:

Accepted for the Council:
Carolyn R. Hodges

Vice Provost and Dean of the Graduate School

(Original signatures are on file with official student records.)

To the Graduate Council:

I am submitting herewith a thesis written by Charles Joel Luckow entitled "New Vibroseis Data and Interpretations from the Shebsh Oil and Gas Field, Southwestern Russia". I have examined the final paper copy of this thesis for form and content and recommend that it be accepted in partial fulfillment of the requirements for the degree of Master of Science, with a major in Geology.

Dr. Richard T. Williams, Major Professor

We have read this thesis and recommend its acceptance:

Dr. Linda C. Kah

Dr. Steven G. Driese

Acceptance for the Council:

Vice Provost and Dean of Graduate Studies

New Vibroseis Data and Interpretations from the Shebsh Oil and Gas Field, Southwestern Russia

A Thesis
Presented for the Master of Science Degree
The University of Tennessee, Knoxville

Charles Joel Luckow
December 2003

ACKNOWLEDGMENTS

I am most grateful for the academic direction of my advisor, Dr. Richard T. Williams, who helped make my two years at the University of Tennessee a rewarding experience. Because of his research in Russia, I was able to participate in an exciting and meaningful thesis project that involved a one-month stay in Russia. My committee members, Drs. Steve Driese and Linda Kah, were very important in making sure deadlines were met and helped with finding useful references. Dr. Bill Dunne devoted half a semester of his Geology 590 class to topics related to my thesis, including fault related folds, foredeeps, and growth strata.

I would like to thank Tengasco Inc. for their generous financial support in the form of the Tengasco Fellowship. With their help I was able to purchase computer equipment, relevant literature, and travel to conferences. I owe much of my future success to their contribution. The University of Tennessee would like to thank the Landmark Graphics Corporation for its contribution of geophysical software used in this thesis. I am appreciative to have received the AAPG Grant-in-Aid (Harold J. Funkhouser Memorial Grant), which was used to fly to Krasnodar, Russia. Acquisition of seismic data for this study was supported by CRDF project REC-004.

Russians who aided in my literature search, translation, and/or the acquisition of the seismic data are: Vladimir Babeshko, Ernest Kutsenko, Vladimir Gulenko, Vladimir Derduga, Alexander Romanov, Serge Popov, Diana Gortinskaya, Natalya Leontyeva, Marina Shulga, and Olga Grishko. University of Tennessee staff and students who especially helped me with UNIX issues are Bill Gray and Jeff Nettles.

Finally, my wife and my parents are owed the greatest thanks. Through useful discussions with my wife, Heather, I better understood the structural and stratigraphic content of my project. My parents, Joel and Linda, are recognized for always supporting and encouraging my academic and professional progress.

ABSTRACT

The Kuban Basin is one of two foredeeps in the northern Caucasus region, southwestern Russia, and has been a significant source of oil and gas in Russia for the past century. In October 2001, The University of Tennessee and Kuban State University acquired new vibroseis data in the Shebsh oil field of the Kuban Basin with the goals of (1) imaging a thrust fault and deeper structures thought to underlie the anticline in the Shebsh field, (2) determining the particular type of fault-related folding that was important during the formation of the anticline, (3) determining the timing of tectonic activity both within the Shebsh oil and gas field and, by inference, elsewhere within the Kuban Basin, and (4) locating prospective hydrocarbon reservoirs within the anticline. An existing interpretation of the structure, based in part on well data and several vintages of older seismic data, depicted it as either a fault-bend or fault-arrest fold with up to 1 km of displacement along a ramp underlying the anticline. The new seismic sections reveal that detachment folding accommodated a major portion of the tectonic shortening. A décollement formed in mechanically weak Paleocene strata that thickened above steeply dipping Cretaceous rocks, which possibly had a buttressing effect during thrusting. Additional tectonic shortening may have been accommodated by the displacement of Paleocene and younger strata up a ramp in fault-arrest folding. Seismic reflector geometries reveal sedimentary thickening on the northeast limb of the anticline, leading to an interpretation that a significant episode of thrusting occurred coeval with sedimentation between ~16 and 7 Ma. The new seismic sections also contain bright spots and high

amplitude reflectors that correlate with interpreted sandstone and limestone layers, and may lead to new drilling targets and increased hydrocarbon production in Eocene, Middle Miocene, and Upper Miocene age strata.

TABLE OF CONTENTS

LIST OF TABLES

LIST OF FIGURES

I. Introduction

Krasnodar Territory, southwestern Russia (Figure 1; all tables and figures can be found in the appendices), is situated in the foreland fold-and-thrust belt of the northern Caucasus Mountains near the Black and Azov Seas. The region is seismically active, but relatively little is known about the seismicity, because no regional seismic network exists at the present time, although efforts are currently underway to install new observatories. It is one of the oldest petroleum-producing regions in Russia, with the first productive well drilled in 1864 (Sudarikov, 1979a, 1979b; Savchenko et al., 2002). Geophysical data including seismic profiles and well logs acquired for petroleum exploration also bear upon fundamental questions about the geology and tectonic evolution of this portion of the orogen. More than 260 individual oil and gas fields have been discovered in the northern Caucasus, with reserves estimated at 200 million tons of oil and 8.75 trillion cubic feet of gas (Sharafan and Markov, 2001). The Shebsh field near the village of Novodmitrievskaya, ~25 km south of the city of Krasnodar, lies within the Kuban Basin (Figure 2), and is one of many in a northwest trending series of oil fields (Figure 3). At least five vintages of seismic reflection data have been obtained in the Shebsh field, from Soviet-era dynamite data to a 3D vibroseis study in 1995, and numerous wells have been drilled, mostly to relatively shallow (<3 km) depths. Nearly all of these data have remained proprietary within the Russian oil and gas industry until now.

The Shebsh field lies adjacent to the northern foothills of the Great Caucasus Mountains. Since initial pulses and throughout subsequent orogenesis, sediment was shed from the rising and eroding orogen. The geometry of sedimentary packages and deformation structures within those packages as revealed by seismic reflection images are useful for interpretation of both timing and type of deformation. In addition, correctly interpreting the deeper structure, beyond the limits of current drilling, will strongly influence future drilling and hydrocarbon production from the Shebsh field.

In October 2001, The University of Tennessee and Kuban State University collected 11 km of 2D vibroseis data in the Shebsh field. The goals of this study were to use new seismic data together with existing seismic data and stratigraphic interpretations of well data to: (1) image a thrust fault believed to underlie the Shebsh field; (2) compare fault-related fold models with the Shebsh anticline to determine its probable type; (3) determine the timing of deformation in this portion of the Kuban Basin; (4) compare the timing of deformation with existing interpretations of tectonic plate motions and regional deformation; and (5) identify locations within the Shebsh anticline that may be most prospective for future hydrocarbon production, by correlating new seismic sections with reservoir rocks observed in existing wells.

II. Location and Geologic Setting

The Great Caucasus Mountains (Figure 2) are a northwest-trending orogen, approximately 1,000 km long, which lies between the Black and Azov Seas to the west and the Caspian Sea to the east (Ershov et al., 1999). The mountain range reaches elevations greater than 5 km above sea level, and is presently undergoing shortening at the rate of 10±2 mm/yr (Reilinger et al., 1997). The orogen (Figure 4) was produced by Alpine deformation during subduction of the Arabian Plate beneath the southern edge of the East European platform. Orogenesis began in the Eocene epoch, reached a maximum during the Miocene epoch, and continues today (Mikhailov et al., 1999).

The northern Caucasus region (Figure 2), also known as the fore-Caucasus or cis-Caucasus, is a foredeep that encompasses approximately 300,000 km^2 (Sharafan and Markov, 2001). There are two distinct basins: (1) the western basin, which is subdivided into the Azov-Kuban Basin in the north and the Kuban Basin in the south, and (2) the eastern basin, where the southern portion is known as the Terek-Caspian Basin. The basins are asymmetrical, deepest adjacent to the orogen and shallowest towards the foreland (Figure 5). An enigmatic crustal feature, the Stavropol High, contains thickened lithosphere and separates the western and eastern foredeeps (Ershov et al., 1999). Whereas the depth to basement is 1-2 km at the Stavropol High, sedimentary rocks attain a maximum thickness of 10-12 km in the Kuban Basin (Figure 4), and the Terek-Caspian Basin is between 12-14 km deep (Polino, 1999).

Compared to other foredeep-orogen pairs, an unusual characteristic of the Great Caucasus foredeep is that the Stavropol High lies adjacent to the topcgraphically highest portion of the orogen, and the greatest subsidence occurred adjacent to the topographically lowest portions of the orogen. The northern Caucasus foredeep is located above the Scythian platform, the southern border of the East European platform, which stretches from the northern border of the Great Caucasus to the northern border of the foredeep (Mikhailov et al., 1999).

III. Petroleum

Petroleum drilling in the Caucasus foreland has steadily increased in depth from a few hundred meters in the 1940's to 3-4 km, and in rare examples to 5-6 km (Sharafan and Markov, 2001). Seismic and well data exist for the upper portion of the sedimentary section, but relatively little data exist for Jurassic and older strata (Mikhailov et al., 1999). Petroleum exploration and drilling by Krasnodar Neftegeofizika, a government agency during Soviet times, took place near Novodmitrievskaya between 1948 and the mid-1980's. The current numbers are proprietary, but as of 1961, 28 wells had been drilled into the Eocene age Kumski horizon, and 31 into the Oligocene-Lower Miocene age Maykop horizon (Voskresenski and Yegolk, 1985).

In recent years, hydrocarbon production and reserves in the northern Caucasus have declined (Figure 6) for two reasons: 1) reductions in capital investment and exploration and 2) depletion of reserves due to ongoing production (Sharafan and Markov, 2001). Curiously, Savchenko et al. (2002) claimed that the possibilities in Krasnodar Territory are exhausted as far as onshore prospects are concerned at a time when the percentage of drilled prospects in the Terek-Caspian and Stavropol fields is 70-95%, but only 5-15% in the Kuban Basin. According to Sharafan and Markov (2001), approximately 50% of the petroleum prospects in the northern Caucasus foredeep have been drilled.

Hydrocarbons are present in strata from Triassic to Miocene-Pliocene age within the Caucasus foreland, but quantitative estimates are unpublished

(Sudarikov, 1979b; Adamia et al., 1991; Popovich, 2001). Triassic, Jurassic, and Cretaceous age complexes have been explored least due to their greater depths (Sharafan and Markov, 2001). Hydrocarbons exist in Jurassic (Callovian) clastic and Oxfordian, Kimmeridgean and Tithonian carbonate strata. Cretaceous strata contain hydrocarbons within the Neocomian sandstone and carbonate strata, and Aptian-Albian sandstone-siltstone complexes (Ulmishek, 2000; Popovich, 2001).

The most explored, drilled, and commercially successful package of sedimentary rock throughout the northern Caucasus, Azov Sea, and Black Sea region has been the Oligocene-Lower Miocene Maykop Formation (Sharfutdinov and Sharfutdinov, 2000; Savchenko et al., 2002). The Maykop Formation consists of interbedded shallow marine sandstones and turbidites, which are reservoir rocks, and marine black shales, which are the source beds. The Maykop Formation lies within the oil window at proto- and mesocatagenic levels, and became mature during the deposition of orogenic clastics between Late Miocene and Pliocene time (Ulmishek, 2000; Popovich, 2001; Savchenko et al., 2002). The formation of oil is related to syntectonic subsidence of the Maykop shales to depths of 2-4 km (Konyuokhov et al., 1999). Maykop shales are also associated with diapiric folds and mud volcanoes. The mud volcanoes and diapiric folds are thought to result from the ascent of water-saturated shales, which were compressed beneath Maykop and younger, orogenically-derived rocks to unknown stratigraphic levels during the Middle to Upper Miocene epochs.

IV. Seismic Reflection Data

Seismic reflection data existing prior to this study included (1) a Soviet-era dynamite line ~25 km long (Figure 7) obtained by Krasnodar Neftegeofizika, and (2) a number of proprietary seismic profiles and 3D data obtained from 1982-1995. Krepenevich and Karrilenko (1995) interpreted these data, together with well data, to show a large anticline possibly underlain by a thrust fault (Figures 7 and 8). New seismic data were acquired in 2001 with the goal of improving the image of the suspected fault and deformation in its footwall, and with a view toward drilling a proposed future well (Figure 8) targeting a hypothesized anticline in the footwall.

A. Acquisition of New Data

Faculty and students from Kuban State University and The University of Tennessee collected vibroseis data for a total distance of 11 km along roads near Novodmitrievskaya (Figure 9) during October and November, 2001. A straight profile perpendicular to strike would have been vastly preferable, but the roads were unpaved and the Russian SV-10/180 vibrator (Figure 10) was not able to operate off-road, on plowed farmland. A Geometrics NX-48 seismograph owned by Kuban State University, together with a roll-switch and a 96-channel roll along cable were used to record the data, simulating a 96-channel acquisition system. A single-ended spread was used with the source pushing the cable. Field recording parameters are summarized in Table 1.

Profile 1 begins in the northeast and extends south along a crooked series of roads (Figure 9) to station 300. Profile 2 starts from the end of profile 1 (station 300) and has the source pushing the cable northeast for a distance of 3.5 km. For processing purposes, profile 1 was separated into two parts, profile 1A from station 1 to 176 and profile 1B from station 176 to 300. An example shot gather from profile 1A is presented in Figure 11 and shows the effect of crooked roads on first arrivals.

B. Seismic Data Processing

The University of Tennessee has a seismic data processing laboratory, based on software donated by the Landmark Graphics Corporation, which includes applications for seismic data processing and interpretation, and well log interpretation. The software used to process the new data was ProMAX, the main seismic data processing application in the Landmark package.

Seismic Unix (SU), a seismic data processing package distributed *gratis* by the Center for Wave Phenomena, Colorado School of Mines, was also used. In particular, geometry information, i.e., shot and receiver coordinates, was initially loaded into the trace headers using SU. A SEG-Y file including the geometry information was written in SU and imported into ProMAX, trace header values were extracted, and geometry assignment was completed in ProMAX. Table 2 summarizes all of the processing steps.

C. Seismic Time Sections

The processed data were projected onto three profiles depending on the direction of the roads (Figure 9). Profiles 1A and 2, both oriented N45°E approximately perpendicular to strike and overlapping to some extent, are presented in Figures 12 and 13, respectively. Profile 1B (Figure 14), oriented north-south, was located near the crest of the anticline based on the observed reflectors, which can be seen dipping gently in both directions along the profile. Importantly, it connects profiles 1A and 2, and establishes the continuity of reflectors between them, allowing profiles 1A and 2 can be displayed in a single time section (Figure 15) after taking the overlap into account.

Referring to profiles 1A and 2 (Figures 12, 13, and 15), strata gently dipping to the northeast are present from the surface to approximately 1.5 s two-way travel time, above a broad anticline evident at 2.2 s and deeper. Also, stratigraphic thicknesses are least above the crest of the anticline, and increase to the northeast. This thickness change is clear from the surface to ~2 s, suggesting that deposition continued coeval with thrusting at least for this interval of geologic time. A bend in the strata, possibly the northeast-vergent thrust fault of Krepenevich and Karrilenko (Figure 8), is visible between 2 s and 3.5 s. The amount of displacement is not obvious, however, and appears to diminish at shallow depths. A number of reflectors, apparently in the footwall of the thrust fault from 3-4 s, cannot easily be correlated with reflectors in the hanging wall. High amplitude reflectors are present in the footwall near 3.3 s and 4.5 s two-way

travel time. The high amplitude reflectors at 3.3 s on the northeastern end of profile 1A suggest a mound-like structure (discussed later). In principle, better resolution of structural details in the footwall of the thrust fault should result from migration of profile 1A. However, attempts at 2D migration, both pre-stack or post-stack, were not successful. Near 3.3 s, antiformal and crossing reflectors are present that migrate at different velocities, suggesting that some of these reflections likely arise outside the plane of the profile, because (1) the data were acquired along crooked roads and (2) the anticline itself is a three dimensional structure. No two-dimensional velocity model will successfully migrate all of the different reflectors. Three-dimensional data, combined with three-dimensional migration, are needed to fully solve the imaging problem.

Referring to profile 2 (Figures 13 and 15), the deepest reflector near 5 s at the southwest end of the profile is particularly interesting. The same reflector can be seen on profile 1B (Figure 14). This reflector, apparently dipping steeply to the south or southeast, is distinctly discordant with the overlying reflectors in the 3.5-4.5 s range, which are subhorizontal to gently dipping. The change in thickness across the profile between the strong subhorizontal reflectors near 3 s and the steeply dipping reflector at 5 s is tectonic in origin, and indicates layer-parallel shortening and possibly the presence of one or more faults subparallel to the reflectors in the 3.5-4.5 s depth range.

V. Well Data

Well data (Figure 16, Table 3) from the Shebsh field were collected and interpreted by workers of Krasnodar Neftegeofizika during the past several decades. Data made available for this study consisted of four types: (1) depth, (2) P-wave interval (layer) velocity from a check shot, (3) geologic age, and (4) lithology. The Stratigraphy Department at Krasnodar Neftegeofizika interpreted geologic age by foraminifera identification. Here, Wells 2, 4, 66, and 530 were used to place seismic reflectors at the correct depth and geologic age, and determine where potential hydrocarbon reservoirs may be located by correlating lithologic interpretations with seismic bright spots and high amplitude reflectors. Data from Ershov et al. (1999) were used to construct a geologic time scale for the western Kuban Basin (Figure 17), including local (Russian) stratigraphic nomenclature.

Well 4 was the most valuable for converting profile 1A seismic data from time to depth, because it is situated directly on the profile and reaches a depth of ~5 km to Paleocene age strata. Velocities in Well 4 (Table 3) were determined at 20 m depth intervals, in contrast to Wells 66 and 530 where velocities were determined at irregular intervals between 10 and 1,000 m. Wells 66 and 530 are important because they lie directly on profiles 1A and 1B, respectively. Well 66 is 2,530 m deep and penetrates the Oligocene-Lower Miocene Maykop Formation. Well 530 is 2,460 m deep and also penetrates the Maykop Formation. Disadvantages of Wells 66 and 530 are their relatively shallow depths and limited

interval velocity information. No well data were available along profile 2. Well 2, a second deep well, lies approximately 4 km east of the Shebsh field and was drilled 5,750 m into Paleocene age strata. Here, it was used indirectly with other wells to help establish the regional stratigraphy.

Well 4 together with a local geologic time scale (Figure 17), was used to construct a depth scale corresponding to two-way travel time, and to correlate seismic reflectors with geologic age. The results are presented in Figures 18-21. A formal time-depth conversion of the seismic traces was not done, because insufficient velocity data were available. Seismic time sections with an approximate depth scale based on information from Well 4 are presented, rather than depth sections.

A major discrepancy exists between the position, in cross-section, of Well 4 on profile 1A (Figure 18) and the existing interpretation (Figure 8) by Krepenevich and Karrilenko (1995). The location of Well 4 in map view is not in doubt. According to the new seismic data, Well 4 should have penetrated the thrust fault/bend in strata at a depth of ~3.9 km, whereas the earlier interpretation, which was based in part on data from the well itself, shows Well 4 to be some distance off the structure to the northeast. Similarly, a discrepancy exists concerning the true depths of Lower Miocene-Oligocene and older rocks. Well 4 is shown in Figure 8 to penetrate the Kumski horizon, an Eocene sandstone, at a depth of ~4.2 km, and there is no fault or repetition of the strata at shallower depths. Based on the new seismic data, the Kumski horizon would

be expected at a depth of ~3.4 km (Figure 22). The discrepancy between the interpretation of seismic profile 1A and the stratigraphic data from Well 4 creates a dilemma. Because the Kumski horizon is the most productive throughout the region, it seems exceedingly unlikely that stratigraphers in the petroleum industry would not recognize it in Well 4, if it is truly present at ~3.4 km. Conversely, the correlation of the strong reflection from the Kumski horizon at ~2 s across the crest of the anticline where it is penetrated by a number of wells (Figure 8) and down the northeast limb (Figures 15 and 22) is compelling.

If it is true that the stratigraphy in Well 4 was incorrectly interpreted, then a similar question can also be raised about Well 2 (Figure 16). Using stratigraphic descriptions from Mikhailov et al. (1999) and Ershov et al. (1999), together with the Russian cross-section, hypothetical, alternative interpretations of Wells 2 and 4 are possible. One such alternative, which is consistent with seismic profile 1A, is presented as 2 CJL and 4 CJL in Figure 16. Here, marker sandstone, limestone, and marl beds from well data presented by Mikhailov et al. (1999) are correlated with similarly positioned beds in Wells 2 and 4. Under this hypothesis, the Kumski sandstone horizon interpreted to lie at ~4.2 km depth (Figure 8) becomes another, older sandstone horizon (Figure 16). The seismic data (Figure 15) provide a strong, but unfortunately not a conclusive, argument that an alternative interpretation of the stratigraphy is needed. Alternately, an as yet unrecognized problem with the seismic data, perhaps related to the crooked

roads and three-dimensional changes in the structure beneath the crooked seismic profile, might account for the apparent dilemma.

VI. Fault-Related Fold Interpretation

Krepenevich and Karnilenko (1995) and the new seismic results are in agreement that the Shebsh anticline is a fault-related fold, but the question of the type of fold remains to be addressed. The major types of fault-related folds are summarized in Figure 23, and each has different implications regarding the stratigraphy that should have been encountered by Well 4.

A fault propagation fold (Figure 23a) occurs when a fold, which may die out in the core of the structure, is situated in front of a propagating fault surface (Suppe, 1985). The base of the system is marked by thrusting, the middle by a faulted fold, and the upper portion by an unfaulted fold (Davis et al., 1983). Strata in the hangingwall travel up a ramp as the fold grows. The ramp does not connect to an upper flat, but is replaced by an asymmetric fold instead. All of the seismic images of the anticline (e.g., Figures 7 and 15) reveal a symmetrical structure, and the steeply dipping forward limb (Figure 23a) of a fault propagation fold is absent.

A detachment fold (Figure 23b) forms above a décollement subparallel to bedding. The space formed between the décollement and the bottom layer of the folded structure is filled by relatively soft, mechanically incompetent rock (Davis et al., 1983; McClay, 1992). A distinctive characteristic of a detachment fold is that the fault does not ramp upward through bedding. Rather, beds are bent and folded (McClay, 1992). Based on the evidence of seismic profile 1A, the Kumski horizon would have been encountered only once in Well 4, at a depth

of ~3.4 km, if the Shebsh anticline is a detachment fold. The subhorizontal décollement would not have been expected at the location of Well 4.

In a fault-arrest fold (Figure 23c), the hanging wall strata travel up a ramp as the fold grows, and the ramp does not connect to an upper flat. The fault continues upward until displacement dies out in the overlying strata. The interpretation by Krepenevich and Karrilenko (1995) shown in Figure 8 is suggestive of a fault-arrest fold or possibly a detachment fold with a secondary, ramped thrust. Based on seismic profile 1A, however, the thrust fault would have been present in Well 4 at a depth of ~3.8 km, and the Kumski horizon would have been repeated at depths of ~3.4 and ~4.2 km. Repetition of strata and the presence of a fault were not found in the interpretation by Krasnodar Neftegeofizika.

A fault-bend fold (Figure 23d) is like a fault-arrest fold, except that the ramp connects to an upper flat. It is clear from both old and new seismic data that the fault, if there is one, continues upward. Thus, a fault-bend fold is not a viable interpretation for the Shebsh anticline.

Given that the fault propagation and fault bend fold models can be ruled out, the question becomes which of the two remaining fold types, detachment (Figure 23b) or fault-arrest (Figure 23c), is the better model for the Shebsh anticline. The models of fault-related folds all involve a well-defined décollement parallel to bedding, which is sub-horizontal as depicted in Figure 23. A possible exception is the detachment fold, where deformation of the mechanically

incompetent rock infilling the space above the décollement is presumably complex. Thomas (2001) has discussed the deformation of shales under similar circumstances, where the formation of the décollement and the forward progress of thrusting were affected by a mechanical buttress, a basement fault, in his examples from the southern Appalachians. In contrast, fault-arrest folding transports strata at constant thickness up a ramp to accommodate tectonic shortening.

The new reflection data (Figure 21) clearly reveal thickening toward the south or southeast of the Paleocene rocks in the 4-7 km depth range. Wells 2 and 4 (Figure 16) and well data from Mikhailov et al. (1999) show that the Paleocene strata are composed primarily of argillite and shale. Numerous reflectors can be found between the Eocene and Cretaceous strata but these all have low amplitude, which implies low acoustic impedance contrasts and thus some degree of mechanical uniformity within the Paleocene section. No obvious reflection from a subhorizontal décollement is visible. Instead, the basal reflector dips steeply south or southeast, and is identified (in the next section) as Cretaceous clastic strata faulted and rotated during an earlier, extensional tectonic event. Jamison (1987) stated that the rheological properties of the strata determine the probable fold-thrust relationship. In this case, detailed information about the rheological properties of the rocks is lacking, and the mechanics are complicated by a possible buttressing effect of the steeply dipping Cretaceous strata, analogous to the situation described by Thomas (2001). Despite such

uncertainties, the seismic data show that a major portion of the tectonic shortening has been accommodated by thickening of the Paleocene strata in the manner of a detachment fold. This observation does not exclude the possibility that some amount of displacement also occurred on a ramp, and thus does not fully resolve the question about whether the structure is better described as a detachment fold or a fault-arrest fold.

The key to understanding the anticline lies in the interpretation of the stratigraphy encountered in Well 4. If the structure is a detachment fold, the Kumski horizon, which is well-known to petroleum geologists in the Kuban Basin, would have been encountered one time, at a depth of ~3.4 km (Figure 22). Alternately, if the structure is a fault-arrest fold and significant displacement is present along the fault, the Kumski horizon would have been encountered two times, at depths of ~3.4 and ~4.2 km, with a fault dipping ~60° in between. It is particularly vexing that the stratigraphic interpretation by Krasnodar Neftegeofizika for both Wells 2 and 4 (Figure 16) is not consistent with either possibility. An interpretation for Well 4 can be constructed (CJL in Figure 16) that is consistent with both a detachment fold and the regional stratigraphy, but it seems unlikely that petroleum geologists who are well acquainted with the Kumski horizon from numerous wells would have misidentified it in Wells 2 and 4.

VII. Tectonics and Identification of Reflectors

Modern theories about the tectonic evolution of the Caucasus region have been presented by Gamkrelidze (1986), Philip et al. (1989), Maslyaev (1990), Ershov et al. (1999), and Mikhailov et al. (1999). Gamkrelidze (1986) based his paleogeographic reconstructions (Figure 24) on geologic, paleomagnetic, paleobiogeographical, paleoclimate data, and the locations of ophiolites. Mikhailov et al. (1999) used 130 wells within the northern Caucasus region to produce subsidence curves. They interpreted the subsidence curves to determine major intervals of uplift in the Great Caucasus and subsidence in the adjacent foredeep. It is not within the scope of this study to reconstruct the paleogeography of the tectonic plates of the Caucasian/Tethyan realm. Instead, the goal is to account for the timing of major events that can be inferred from the seismic data in the context of existing theories about the tectonic evolution.

The formation of the present-day tectonic structure of the Caucasus region began in the Carboniferous period when the Transcaucasian Plate (Figure 24a), a microcontinent or island arc, moved north and was subducted beneath the East European platform. The collision produced calc-alkaline volcanics and closed a portion of the Tethys Ocean known as the northern or Paleotethys Ocean. The Iran-Afghan and Arabian Plates began to move northward, which formed a southern or Mesotethys Ocean. At the end of the Paleozoic Era, the Anatolian Plate separated from Africa and was moving northward (Gamkrelidze, 1986).

Permian age Hercynian metamorphic basement, consisting of schist and igneous rocks, lies beneath the northern Caucasus foredeep. The basement is also known as the Scythian platform, and is the southern edge of the Russian or East European platform. Sedimentary cover above Hercynian basement begins with Triassic age rocks and continues through Pliocene-Quaternary at the surface. The northern Caucasus foreland is thought to have originated as a Triassic rift basin, but most of the Triassic strata, composed of volcano-clastic, carbonate, and clastic rocks, were eroded during the Cimmerian Orogeny (Late Triassic-Late Jurassic), which was a collisional event between the Laurasian, Cimmerian, and southeast Asian plates (Mikhailov et al., 1999).

The Paleotethys Ocean closed in the Jurassic period (Figure 24b) as the Iran-Afghan Plate docked against the East European platform (Gamkrelidze, 1986). The lithosphere in the northern Caucasus region at this time is thought to have been inhomogeneous, with the Stavropol High having thicker lithosphere than the eastern and western regions. The Scythian platform subsided between the Jurassic and Cretaceous periods (Mikhailov et al., 1999). Eastern and western deep sedimentary basins formed, and a wide, shallow basin formed in between. Platform cover was deposited on the Scythian platform beginning in the Middle Jurassic period and continued until the Eocene epoch. The platform was a shelf margin of a deep-water, back arc basin (Mikhailov et al., 1999; Scotese, 2003). The Middle Jurassic succession is made up of sandstones and marine argillites with an aggregate thickness of 1.3 km. The Late Jurassic

(Oxfordian) sequence is composed of carbonate platform sediments with interbedded clay up to 0.25 km thick (Mikhailov et al., 1999).

The origin of the Black Sea remains enigmatic, but it is thought to have developed between the Jurassic period and Paleocene epoch, after the closure of the Paleotethys Ocean. The region was a shallow basin between the Mesozoic era and Paleogene epoch. During Alpine orogenesis (Oligocene-Miocene), regional depressions formed due to tectonic loading of the lithosphere by the Caucasus Mountains. Such depressions may have connected, forming larger basins. During the Pliocene epoch, the Black Sea was a deep-water depression that continued to subside (Shirshov, 1980). Smolianinov et al. (1996) stated that the Black Sea is either (1) a remnant of the Tethys Ocean, where the Anatolian Plate separated it from the rest of the Tethys Ocean or (2) a remnant of a back-arc basin formed in the Late Mesozoic-Early Tertiary periods.

A subduction zone formed during the Cretaceous (Figure 24c) on the southern edge of the Iran-Afghan Plate, which emplaced ophiolites and produced volcanism that persisted until the Cenozoic. The Anatolian Plate moved northward and closed a basin between itself and the East European platform. The Arabian Plate underthrust the Iran-Afghan Plate, which produced Late Cretaceous-Cenozoic volcanism in the Iran-Afghan Plate (Gamkrelidze, 1986). Between the Late Cretaceous period and the Middle Eocene epoch, subsidence in the western basin occurred at a higher and faster rate than the eastern domain, probably caused by a change in the arrangement of plate boundaries

(Mikhailov et al., 1999). The Lower Cretaceous strata are made up of glauconitic sandstone and clay with thicknesses from 1.5-1.7 km. Clastic rocks having a thickness of ~0.6 km comprise the Upper Cretaceous succession (Mikhailov et al., 1999). Well data (Figure 16) indicate that argillites makeup Paleocene age strata, thus seismic sections lack prominent reflectors in the Eocene and Cretaceous intervals (Figures 18-20).

The prominent, steeply dipping reflectors between 6-7 km revealed by the new seismic sections (Figure 21) are interpreted to be Cretaceous age clastic rocks, based on stratigraphic descriptions and depths given by Mikhailov et al. (1999), although existing wells near Novodmitrievskaya do not reach Cretacecus strata. According to Derduga (2003), post-Cretaceous extension produced high-angle normal faults, horsts and grabens, and thus created a basin, which was the precursor to the modern Kuban Basin. His description is consistent with the regional cross section (Figure 5) by Burshtar et al. (1966), but a search of the Russian literature did not yield any additional, specific information about the extensional tectonic event.

During the Eocene epoch (Figure 24d), oceanic crust was formed in a rift zone in the Black Sea region (Gamkrelidze, 1986; Mikhailov et al., 1999). Mikhailov et al. (1999) claimed that subsidence curve interpretations point towards the formation of the Black and Caspian Seas in the Early Paleocene epoch. Andesite and dacite volcanics were produced in the Lesser Caucasus caused by the subduction of both the Arabian and Anatolian Plates. Deposition

of pre-orogenic carbonates in both the Lesser and Great Caucasus region ended in this period and post-orogenic sediments accumulated, which is evidence that the orogen was rising (Gamkrelidze, 1986). Shallow-water carbonates and marls were deposited in the basin between the Paleocene and Eocene (65-34 Ma) epochs (Ershov et al., 1999). The time period between the Middle Eocene and the present is characterized by the formation of the northern Caucasus foredeep, caused by the uplift of the Great Caucasus Orogen. Periods of short uplift and longer subsidence took place, based on interpreted subsidence curves. 1.5-2 km of fine-grained clastics and shales comprise the Paleocene-Eocene strata (Mikhailov et al., 1999). The most prominent reflector in the seismic sections is the sandstone Eocene Kumski horizon. Shales make up most of the Eocene age stratigraphy.

Enigmatic reflectors are present at 3.3 s (4.3 km) near the northeastern end of profile 1A (Figures 12 and 18). They are mound-like, and were not amenable to 2D migration. Shanmugam and Moiola (1988) said that mounded seismic reflections are regularly indicative of fan lobes, and defined submarine fans as channel and lobe complexes produced by sediment-gravity flows in deep water beyond the continental shelf. These develop during a global lowstand of sea level, and make for favorable hydrocarbon reservoirs, because they are primarily composed of channel-fill, quartz-rich sandstones, are laterally continuous, and have high porosity. The interpretation of logging data from Well 4 at Krasnodar Neftegeofizika (Figure 16) placed the Kumski horizon at 4.3 km

depth, the depth of mound-like reflectors. Absent additional information, for example samples of the rocks from Well 4 or 3D seismic data, it is not possible to conclude that the mound-like reflectors are a part of a low-stand fan complex.

Post-Eocene time is considered to represent the orogenic phase of the Great Caucasus and the period of most deformation within the northern Caucasus foredeep (Maslyaev, 1990). Deep-water shales and interbedded sandstones comprise the Oligocene-Lower Miocene age Maykop Formation in the Kuban Basin and in some locations attain thicknesses of 1.7 km (Ershov et al., 1999). Seismic profiles (Figures 18-20) show bright reflectors between dim sections, consistent with well interpretations of interbedded sandstone layers. The Middle Miocene epoch is considered to be the peak of orogenesis in the Great Caucasus. Between the Late Oligocene-Early Miocene (34-16 Ma) epochs, intense downwarping of the crust occurred and the Kuban and Terek-Caspian Basins continued to deepen by approximately 3 km. Changes in thickness of Maykop sediments indicate changes in the direction of tectonic movements. Coarse-grained gravel accumulated in the southern portion of the Kuban Basin during this period. Between the Middle-Upper Miocene and Middle Pliocene epochs, the Azov-Kuban Basin (northern portion of the western foredeep) subsided (Maslyaev, 1990). The Great Caucasus, as a whole, were subaerially exposed by the Middle-Upper Miocene (12.2-9.3 Ma; Middle-Late Sarmatian), whereas the central Great Caucasus had been exposed above the sea since the Eocene. After 9.3 Ma (Late Sarmatian; Upper Miocene), the

Stavropol High remained static, while the eastern and western basins continued to subside. The Kuban and Terek-Caspian Basins deepened near the orogen and were infilled with carbonates and clastics derived from the Great Caucasus. Shallow-water clastic sediments with interbedded limestones and lagoon deposits characterize Middle Miocene strata, which have a thickness ranging from 0.7-1 km in the Kuban Basin. Upper Miocene interbedded limestones and shales comprise 1.2 km of strata (Mikhailov et al., 1999). Seismic sections (Figures 18-20) display prominent reflectors in Miocene-Quaternary age strata and correlate with sandstone and limestone layers from well data.

The Black Sea and Caspian Seas were separated at the end of the Miocene (6.0-5.2 Ma) as sea level dropped significantly. Rivers incised the foredeep beginning in the Early Pliocene (5.2-3.4 Ma). Pliocene-Quaternary age deposits in the Kuban Basin are sandstone, conglomerate, and marine and continental clastics with thicknesses ranging from 1-1.2 km (Ershov et al., 1999).

Mikhailov et al. (1999) concluded, via paleobathymetric and subsidence curve interpretations, that there were four major stages of tectonism that formed the Great Caucasus and the adjacent foredeep. The basis for their conclusions is that pulses in orogenesis bring about phases of subsidence of foredeep strata. The stages are the Late Eocene (39.5-36 Ma), Middle Miocene (Chokrakian-Karaganian; 16.6-15.8 Ma), Middle Miocene (Konkian-Sarmatian; 14.3-12.3 Ma), and Upper Miocene (Pontian; 7.0-5.2 Ma). The present-day structure of the foredeep formed during the Middle-Upper Miocene (Sarmatian in Figure 17). In a

contrasting view, Philip et al. (1989) suggested that the Arabian Plate initially collided with the East European platform at 3.5 Ma (Middle Pliocene). Results of collision were the ejection of the Anatolian Plate westward, and the Iran-Afghan Plate eastward. As the Arabian Plate moved northward against the platform, the Lesser Caucasus collided with the crust to the north, thereby causing the most significant uplift of the Great Caucasus.

The present-day Arabian Plate (Figure 4) is traveling at approximately 25±3 mm/year, which is causing 10±2 mm/year of crustal shortening in a north-south direction, based on differential GPS estimates (Reilinger et al., 1997). Ongoing tectonic activity was recently evidenced on November 9, 2002, when a magnitude 5.0 earthquake occurred 35 km NNW of the major Black Sea port city Novorossisk (Figures 1 and 2) (U.S.G.S. Earthquake Hazards Program, 2002).

VIII. Discussion

A. Timing of Deformation

Profile 1A (Figure 18) is the most useful of the three profiles for constraining the time when deformation ceased in the Shebsh anticline, because it displays stratigraphic thickening or growth strata (sediment deposited coeval with thrusting) in the northeastern portion of the profile. Figure 25 depicts an idealized model by Suppe et al. (1992) of pre-growth and growth strata, and is similar to the pattern seen in the Shebsh anticline (Figures 12 and 18). Sedimentary packages that display thickening delimit when tectonism was active, and packages that are not thickened delimit when tectonic stability dominated.

The sedimentary geometries of Chokrakian-Meotian (Middle and Upper Miocene, ~16-7 Ma) (Figure 17) age rock show a thickening from southwest to northeast. Thickening is evident in both interpreted seismic sections and well data (Figures 12, 15 and 16) and is interpreted to result from growth strata. Eocene-Oligocene strata do not display stratigraphic thickening from the south to north and are interpreted to be pre-deformation strata. Pontian and Pliocene-Quaternary strata also appear stratigraphically unthickened, and are interpreted to be post-deformation strata.

Local deformation in the Shebsh field is interpreted to have occurred after the Oligocene and during the Chokrakian-Meotian interval, based on the sedimentary geometries. Because strata packages are not thickened, Pontian and Pliocene-Quaternary age strata are interpreted to have been deposited

during a time of relative tectonic stability. The interpreted timing of deformation roughly correlates with Miocene age deformational pulses described by Mikhailov et al. (1999). Although they describe three phases of deformation, the interpretation presented here begins during their second phase (16.6-15.8 Ma) and ends at the beginning of their fourth phase (7-5.2 Ma).

B. Prospective Hydrocarbon Reservoirs

Bright spots and high amplitude reflectors are visible in the seismic sections. Bright spots are localized seismic amplitude anomalies that can indicate the presence of hydrocarbons under favorable circumstances. They result from changes in acoustic impedance, possibly in connection with changes in lithology or fluid content. Here, bright spots and high amplitude reflectors on the seismic sections are correlated with interpreted sandstone and limestone layers from the well data (Figure 16) to determine where hydrocarbon reservoirs and thus promising drilling targets may exist.

The Eocene age Kumski horizon, composed primarily of sandstone, is consistently associated with high amplitude reflections, and locally produces bright spots. The most striking bright spots are displayed in profiles 1B and 2 near the crest of the anticline (Figures 13 and 14). Lower amplitude reflections can be seen on the northeast side of the anticline in profile 1A (Figure 26a), suggesting that hydrocarbons possibly migrated from lower stratigraphic levels to the crest of the anticline. Bright horizons correlate with Lower Eocene

sandstones at ~4.2 km depth in profile 1A (Figure 26a) and 3.5-3.9 km in profiles 1B and 2 (Figures 26b and 26c).

Referring to Figures 26a and 26b, Lower and Upper Sarmatian (Middle Miocene) sandstones correlate with high amplitude reflections at 1.6 and 1.9 km in profile 1A, and at 1.3 km in profile 1B. Pontian and Meotian (Upper Miocene) horizons also show bright reflectors and correlate with sandstones. Chokrakian (Middle Miocene) and Pontian (Upper Miocene) limestones in profile 1A correlate with bright reflectors at 2.4 and 1.1 km, respectively. A structural trap may be present in one of the Chokrak horizons at 2.4 km near Well 4. Trace amplitudes appear to increase in the horizon towards the fault or bend in strata. Upper Chokrakian-Lower Karaganian (Middle Miocene) sandstones correlate with several bright reflectors at 1.7 km in profile 1B. Pliocene-Quaternary sand correlates with a bright spot at 0.5 km in profile 1B. The Pliocene-Quaternary sedimentary rocks may be too young and/or too shallowly buried for hydrocarbons to have matured.

IX. Conclusions

1. Both detachment folding and fault-arrest folding may have contributed to the formation of the Shebsh anticline. Thickened, mechanically weak Paleocene strata above south or southeast dipping Cretaceous clastic rocks shows that detachment folding accommodated a major portion of the tectonic shortening. Speculatively, pre-existing dip of the Cretaceous strata may have had a buttressing effect during thrusting, and contributed to the development of a décollement in the overlying Paleocene strata. The existing seismic data do not resolve the amount of additional tectonic shortening that movement of Paleocene and younger strata up a ramp may have accommodated in the manner of fault-arrest folding.
2. The key to improving the interpretation lies in (i) acquiring new three-dimensional seismic data along straight lines, to overcome possible objections to the existing seismic images, which are based on crooked line data; and (ii) a review of the well data, particularly from Wells 2 and 4, to determine whether the Kumski horizon can be identified at a depth of ~3.4 km, and is possibly repeated at a depth of ~4.2 km.
3. Interpretations of stratal geometries suggest that deformation related to orogenesis in the northern Caucasus foreland began in the Middle Miocene (16 Ma) and ended in the Upper Miocene (7 Ma). These dates correlate with interpretations by Mikhailov et al. (1999) of pulses in tectonism.

4. Bright spots and high-amplitude reflectors indicate that hydrocarbon reservoirs may exist predominantly in Eocene, Middle Miocene, and Upper Miocene sandstone layers and Middle Miocene limestone layers, and that numerous new targets exist for future drilling.

References Cited

References Cited

Adamia, S.A., Akhvlediani, K., Chabukiant, A., and Kilasonia, V., 1991, The Caucasian oil and gas province: AAPG Bulletin, v. 75, no. 8, p. 1401.

Burshtar, M.S., Biznegayev, A.D., Gasangusenov, G.G., Znamenskeya, V.A., Korotkov, S.T., Maksemov, S.P., Pustelsnekov, M.P., 1966, Geology of the oil and gas deposits of the northern Caucasus, Moscow, p. 32.

Davis, D., Suppe, J., and Dahlen, F.A., 1983, Mechanics of fold-and-thrust belts and accretionary wedges: Journal of Geophysical Research, v. 88 p. 1153-1172.

Ershov, A.V., Brunet, M.F., Korotaev, M.V., Nikishin, A.M., and Bolotov, S.N., 1999, Late Cenozoic burial history and dynamics of the Northern Caucasus molasse basin: implications for foreland basin modeling: Tectonophysics, v. 313, p. 219-241.

Gamkrelidze, I.P., 1986, Geodynamic evolution of the Caucasus and adjacent areas in Alpine time: Tectonophysics, v. 127, p. 261-277.

Jamison, W.R., 1987, Geometric analysis of fold development in overthrust terranes: Journal of Structural Geology, v. 9, n.2, p. 207-219.

Konyukhov, A., Sokolov, B., and landrebiev, N., 1999, Geological evolution of the Precaucasus hydrocarbon basins: European Union of Geosciences conference abstracts, Journal of Conference Abstracts, Cambridge Publications. Cambridge, United Kingdom, v. 4, n. 1, p. 326.

Krepenevich, V.L., and Karrilenko, V.I., 1995, Unpublished interpretation of the anticline underlying the Shebsh field. Vasiliy Lavrentievich Krepenevich (deceased) was Chief Geologist of Krasnodar Neftegeofizika. Vitaliy Ivanovich Karrilenko (deceased) was Chief of the Geological Department "MGDY" Chernomorneft, a petroleum company operating the Shebsh field.

Kutsenko, E., 2002, Personal communication in Krasnodar, Russia.

Maslyaev, G.A., 1990, The specifics of the Fore-Caucasus structure formation at the Cenozoic (in Russian): Geotectonics, v. 4, p. 52-60.

McClay, 1992, Thrust Tectonics, Chapman & Hall, London, p. 428.

Mikhailov, V.O., Panina, L.V., Polino, R., Korronovsky, N.V., Kiseleva, E.A., Klavdieva, N.V., and Smolyaniova, E.I., 1999, Evolution of the North

Caucasus foredeep: constraints based on the analysis of subsidence curves: Tectonophysics, v. 307, p. 361-379.

Philip, H., Cisernas, A., Gvishiani, A., and Gorshkow, A., 1989, The Caucasus: an actual example of initial stages of continental collision: Tectonophysics, v. 161, p. 1-21.

Polino, R., 1999, Caucasus: Geodynamics of Collision-Related Basins: http://www.geofys.uu.se/eprobe/Projects/caucasus/Caucasus.htm.

Popovich, S.V., 2001, Geologic basis for oil-gas potential of northeast part of Black Sea: Petroleum Geology, v. 35, n. 3, p. 227-236.

Reilinger, R.E., McClusky, S.C., Souter, B.J., Hamburger, M.W., Prilepin, M.T., Mishin, A., Guseva, T., and Balassanian, S., 1997, Preliminary estimates of plate convergence in the Caucasus collision zone from global positioning system measurements: Geophysical Research Letters, v. 24, n. 14, p. 1815-1818.

Savchenko, V.I., Glebov A.Y., and Popovich, S.V., 2002, Problems in geological study and exploration for oil and gas in Azov-Black Sea region: Petroleum Geology, v. 36, n. 4, p. 348-352.

Scotese, C., 2003, www.scotese.com/earth.htm

Shanmugam, G., and Moiola, R.J., 1988, Submarine fans: Characteristics, models, classification and reservoir potential: Earth Science Reviews, v. 24, p. 383-428.

Sharafan, V.Y. and Markov, A.N., 2001, Structure and potential for oil-gas exploration in the North Caucasus: Petroleum Geology, v. 35, n. 4, p. 378-381.

Sharfutdinov, F.G. and Sharfutdinov, V.F., 2000, Geology and Oil-Gas Prospects of Maykop Sediments of East Cis-Caucasus, Petroleum Geology, v.34, 2, p. 118-125.

Shirshov, P.P., 1980, The geological history of the Black Sea based on the results of deep-water drilling: Academy of Science, USSR, Institute of Oceanography, p. 188-189.

Smolianinov, E.I., Mikhailov, V.O., and Lyakhovsky, V.A., 1996, Numerical Modeling of the regional neotectonic movements in the northern Black Sea: Tectonophysics, v. 266, p. 221-231.

Sterner, R., 1998, members.tripod.com/~argun/region_6.htm.

Sudarikov, A., 1979a, Oil-Gas Region of the Azov-Kuban Depression: Petroleum Geology, v. 17, p. 170-171.

Sudarikov, A., 1979b, North Caucasus Oil-Gas Province: Petroleum Geology, v. 17, p. 172-173.

Suppe, J., 1985, Principles of Structural Geology, Prentice-Hall, Inc., Englewood Cliffs, New Jersey, p. 537.

Suppe, J., Chou, G.T., and Hook, S.C, 1992, Rates of folding and faulting determined from growth strata, in: K.R. McClay, ed., Thrust Tectonics, Chapman and Hall, p. 105-121.

Thomas, W. A., 2001, Mushwad: Ductile duplex in the Appalachian thrust belt in Alabama: AAPG Bulletin, v. 85, no. 10, p. 1847-1870.

Thorbjornsen, K.L., and Dunne, W.M., 1997, Origin of a thrust-related fold: geometric vs. kinematic tests: Journal of Structural Geology, v. 19, p. 303-319.

Ulmishek, G.F., 2000, Azov-Kuban Basin (1108): U.S. Geological Survey World Petroleum Assessment 2000.

U.S.G.S. Earthquake Hazards Program, 2002, neic.usgs.gov/neis/bulletin/neic_lhhm_w.html.

Voskresenski, I.A. and Yegolk, V.L., 1985, Catalog of Stratigraphical Cross-Sections of Krasnodar Territory Wells, Ministry for the Oil Industry, Krasnodar, Russia.

Williams, G., and Chapman, T., 1983, Strains developed in the hangingwalls of thrusts due to their slip/propagation rate; a dislocation model: Journal of Structural Geology, v. 5, no. 6, p. 563-571.

Appendices

Appendix 1

Tables

Table 1. Field recording parameters during seismic acquisition.

Parameter	Value
Sweep:	10-100 Hz for 18 seconds
Listening time:	24 seconds
Correlated record length:	6 seconds
Sweeps per shot point:	10
Number of channels:	96 (simulated by 48x2 channel records
Sample interval:	2 ms
Filters:	50 Hz and 150 Hz notch
Nominal group (receiver) interval:	26.5 m
Nominal source interval:	53 m
Nominal stacking fold:	48

Table 2. Seismic data processing steps.

Step	Description
Geometry Assignment-Header Load:	Combines spatial coordinates with the seismic data.
Datum Statics:	Correction that compensates for shots and receivers at different elevations.
True Amplitude Recovery:	Applies a gain function to compensate for loss of energy due to attenuation of the seismic wave.
Kill Dead Traces:	Delete seismic traces that show excessive noise.
Velocity Analysis (Semblance):	A tool used to estimate stacking (NMO) velocities.
Normal Moveout Correction:	Simulates zero-offset data, as if the vibrator were collocated with the geophone.
Automatic Gain Control:	A method of scaling all trace amplitudes.
CDP Stack:	Produces the completed seismic time section.

Table 3. Depth versus interval velocity from Well 4, used to convert two-way time to depth. Well 4 only describes interval velocity to 5 km. Below 5 km estimated velocities were used. Kutsenko, 2002.

Depth (m)	Interval Velocity (m/s)	Depth (m)	Interval Velocity (m/s)	Depth (m)	Interval Velocity (m/s)
20		800	2420	1580	2830
40		820	2200	1600	2495
60	1820	840	2445	1620	2890
80	1975	860	2590	1640	2760
100	1860	880	2125	1660	2955
120	1770	900	2485	1680	2780
140	1740	920	2420	1700	2780
160	1715	940	1980	1720	2645
180	1830	960	2300	1740	2620
200	1910	980	2110	1760	2850
220	1865	1000	2210	1780	2955
240	1940	1020	2535	1800	2800
260	1975	1040	2400	1820	2705
280	2060	1060	2250	1840	2725
300	2215	1080	2580	1860	2710
320	2210	1100	2470	1880	3170
340	2250	1120	2630	1900	3440
360	2340	1140	2740	1920	3080
380	1985	1160	2500	1940	3105
400	1945	1180	2500	1960	2915
420	2240	1200	2435	1980	2800
440	1900	1220	2415	2000	2970
460	2210	1240	2220	2020	2810
480	2310	1260	2240	2040	2805
500	2080	1280	2415	2060	2775
520	2380	1300	2270	2080	2775
540	2235	1320	2450	2100	2875
560	2190	1340	2620	2120	2905
580	2220	1360	2340	2140	3170
600	2070	1380	2755	2160	2735
620	2185	1400	2730	2180	2950
640	2300	1420	2260	2200	2675
660	2120	1440	2410	2220	2580
680	2175	1460	2280	2240	3135
700	2255	1480	2150	2260	2580
720	2015	1500	2380	2280	2895
740	2260	1520	2685	2300	2620
760	2060	1540	2770	2320	2655
780	2090	1560	2750	2340	2835

Table 3 (continued). Depth versus interval velocity from Well 4, used to convert two-way time to depth. Well 4 only describes interval velocity to 5 km. Below 5 km estimated velocities were used. Kutsenko, 2002.

Depth (m)	Interval Velocity (m/s)	Depth (m)	Interval Velocity (m/s)	Depth (m)	Interval Velocity (m/s)	Depth (m)	Interval Velocity (m/s)
2360	2875	3140	3315	3920	2605	4740	3490
2380	2875	3160	3275	3980	2555	4760	3390
2400	2630	3180	3290	4000	2540	4780	3360
2420	2930	3200	3120	4020	2615	4800	3350
2440	2815	3220	3210	4040	2660	4820	3375
2460	3315	3240	3715	4060	2650	4840	3670
2480	3050	3260	3160	4080	2795	4860	4125
2500	3060	3280	3185	4100	3005	4880	4445
2520	3075	3300	3050	4120	3240	4880	4445
2540	2805	3320	2690	4140	3450	4900	4735
2560	3170	3340	2960	4160	3520	4920	4910
2580	2995	3360	2960	4180	3290	4940	4880
2600	2795	3380	3075	4200	3200	4960	4520
2620	2795	3400	3290	4220	3040	4980	4650
2640	2675	3420	3430	4240	3040	5000	4700
2660	2680	3440	3535	4260	3150		
2680	2555	3460	2910	4280	3200		
2700	2760	3480	2950	4300	3360		
2720	2660	3500	3275	4320	3360		
2740	2540	3520	3185	4340	3305		
2760	2630	3540	3665	4360	3265		
2780	2387	3560	3300	4380	3225		
2800	2400	3580	2995	4400	3240		
2820	2460	3600	2855	4420	3265		
2840	2520	3620	2805	4440	3250		
2860	2805	3640	2760	4460	3225		
2880	2770	3660	2740	4480	3185		
2900	2655	3680	2825	4500	3275		
2920	2785	3700	2895	4520	2785		
2940	2385	3720	2805	4540	2785		
2960	2655	3740	2630	4560	2910		
2980	2650	3760	2630	4580	2810		
3000	2460	3780	2580	4600	3320		
3020	2805	3800	2590	4620	3490		
3040	2640	3820	2630	4640	3320		
3060	2825	3840	2640	4660	3460		
3080	3120	3860	2615	4680	3490		
3100	3120	3880	2620	4700	3415		
3120	3290	3900	2710	4720	3540		

Appendix 2

Figures

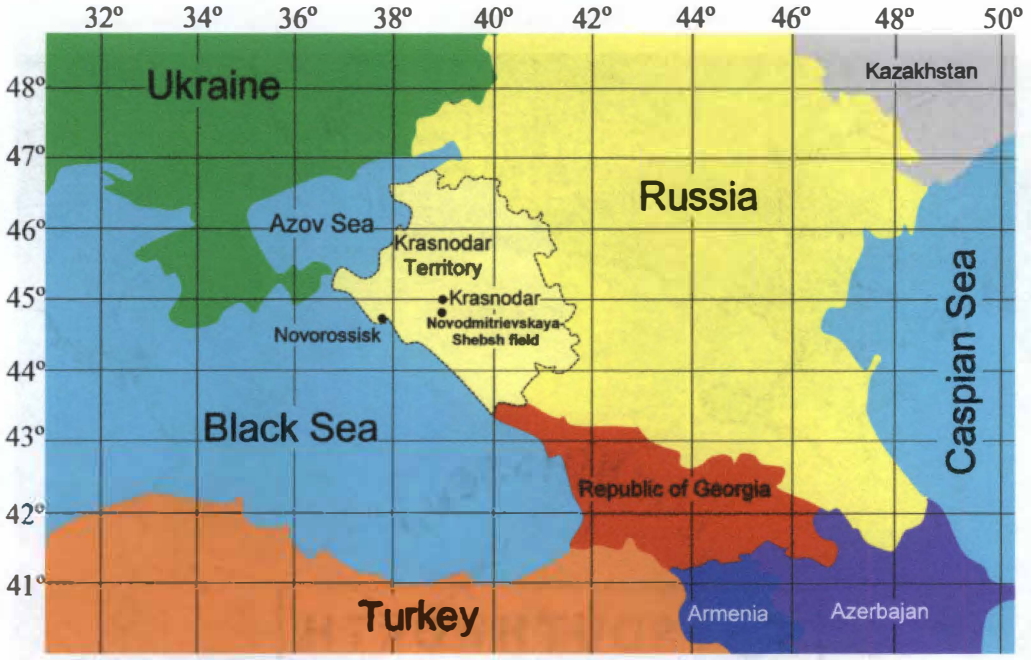

Figure 1. Map showing southwestern Russia, Krasnodar Territory, and surrounding countries. The Shebsh oil and gas field near Novodmitrievskaya is located south of Krasnodar at 45°N latitude and 39°E longitude. Novorossisk is a major Black Sea port city that experienced a magnitude 5.0 earthquake in November 2002.

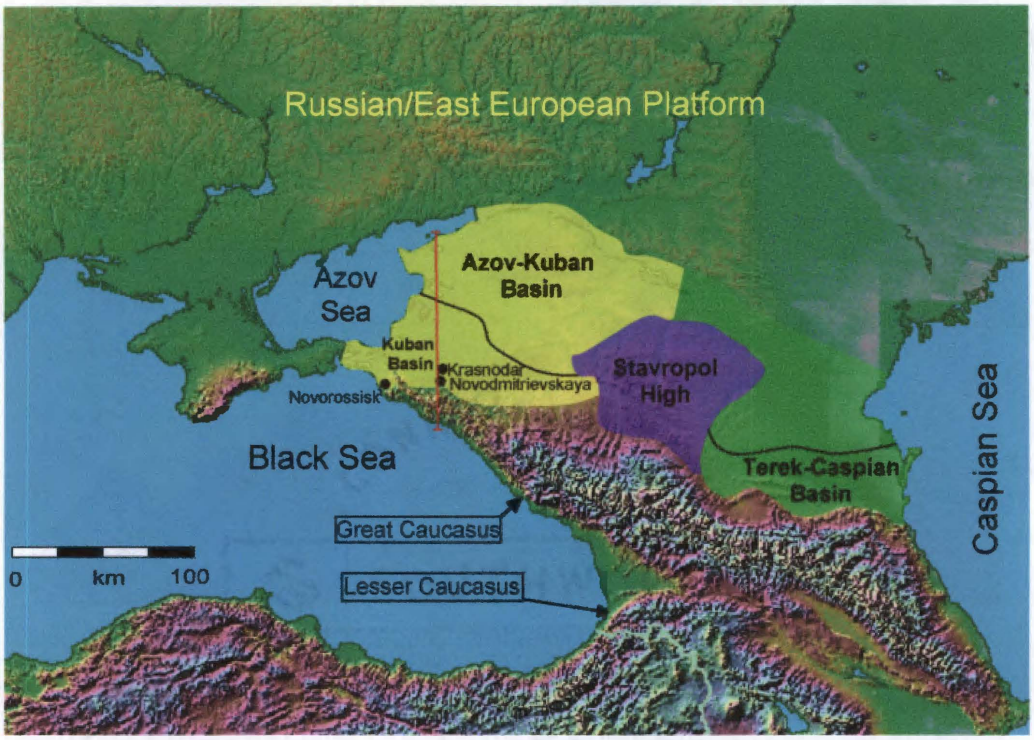

Figure 2. Principle tectonic components of the Caucasus foreland. Shown are the western foredeep and Kuban Basin (yellow); eastern foredeep and Terek-Caspian Basin (green); and Stravropol High (purple). Red line shows location of the cross-section in Figure 5. Outline of foredeeps modified from Ershov et al. (1999); Pseudotopographic image from Sterner (1998).

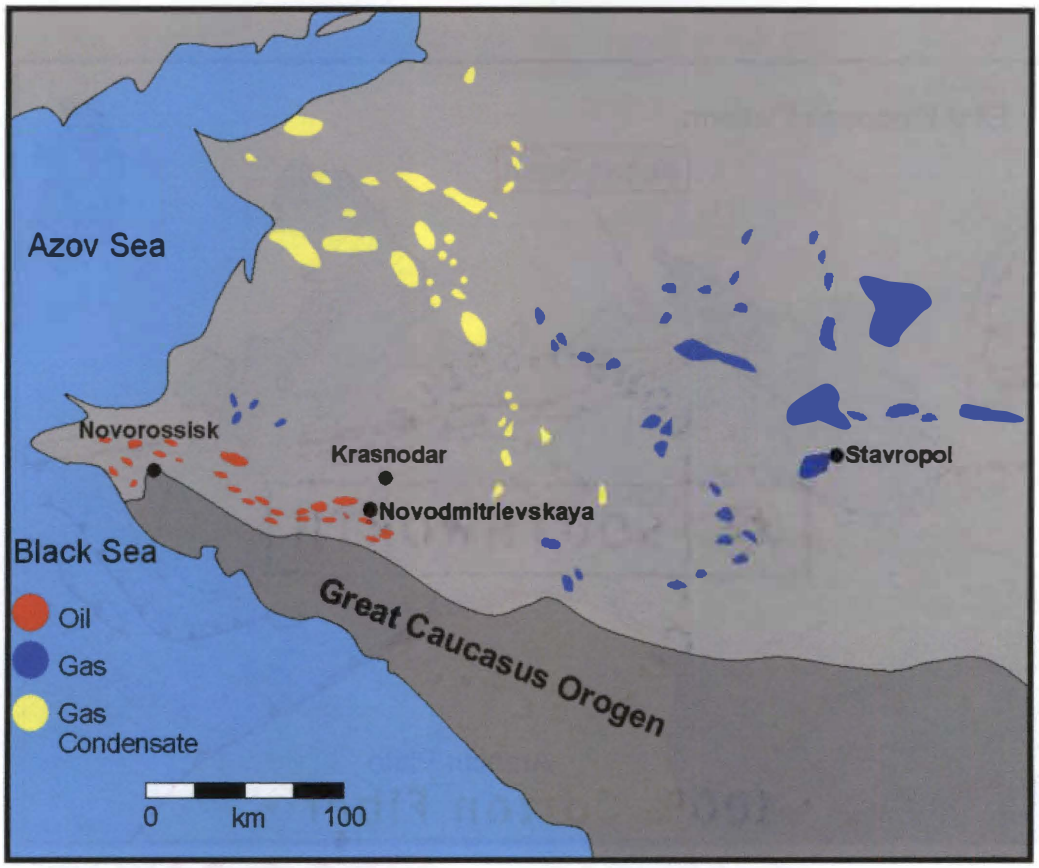

Figure 3. Known oil, gas, and gas-condensate sites of the northwestern Caucasus region. Modified from Burshtar et al. (1966).

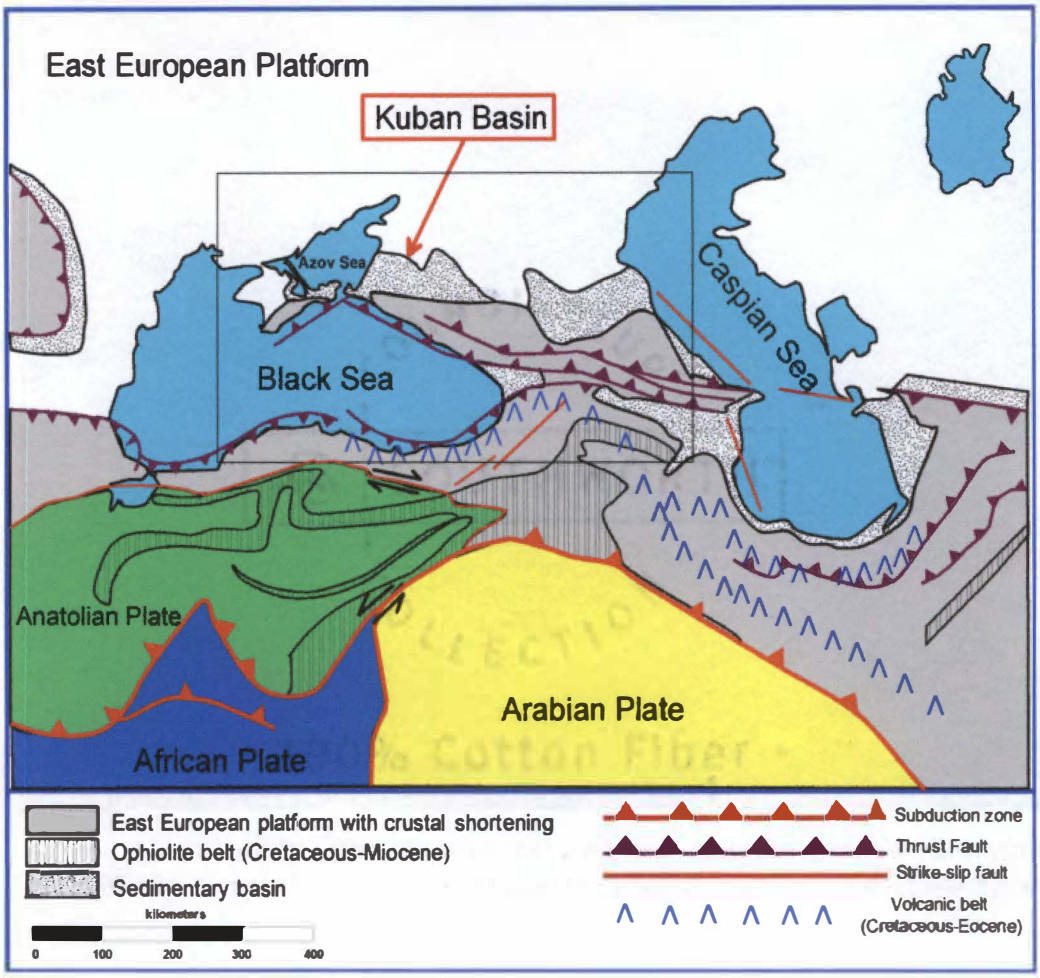

Figure 4. Modern tectonic setting of the Caucasus region. Black box outlines the area shown in Figures 1 and 2. Modified from Ershov et al. (1999).

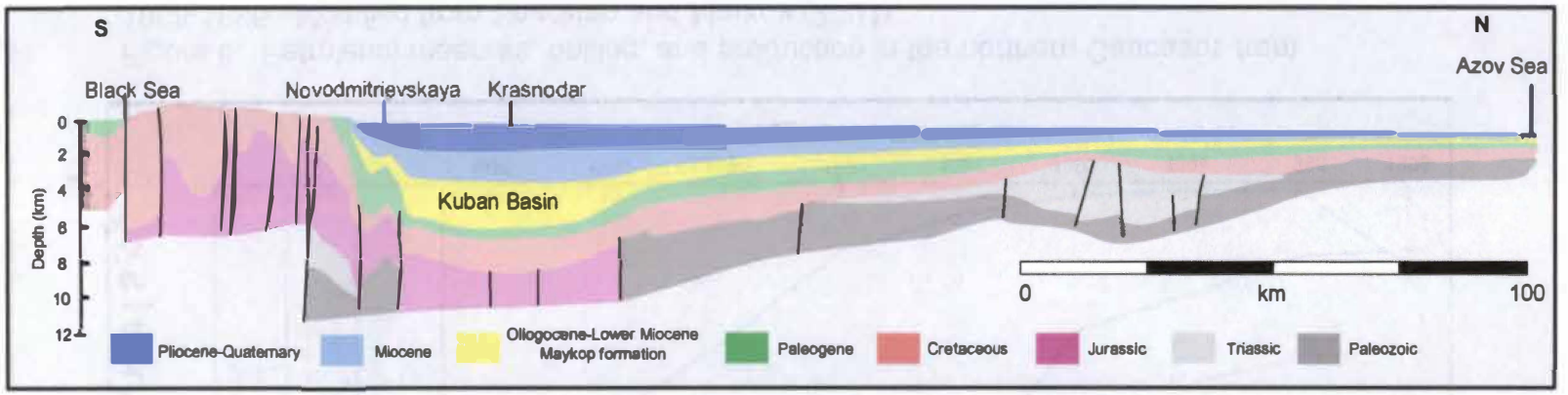

Figure 5. Regional cross-section based on well data and deep seismic soundings. The profile (red line in Figure 2) runs from the Black Sea, through the northern Caucasus, to the Azov Sea. Modified from Burshtar et al. (1966).

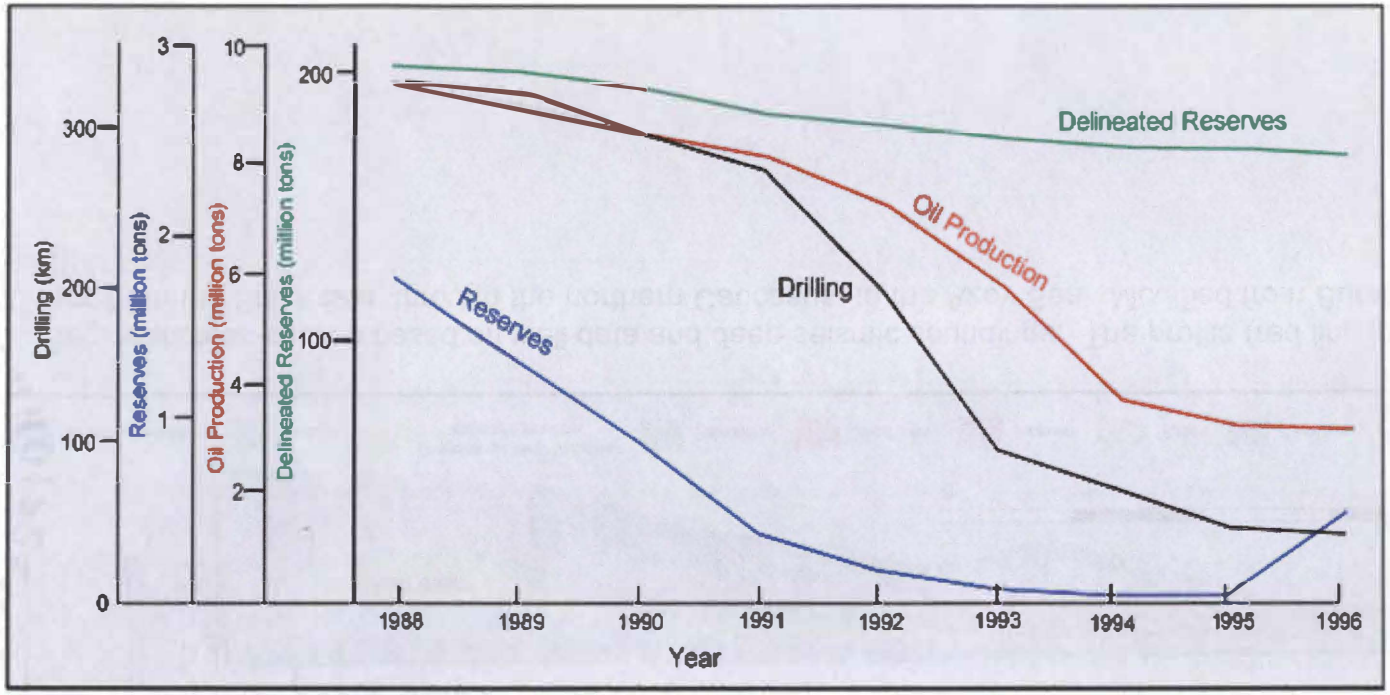

Figure 6. Petroleum reserves, drilling, and production in the northern Caucasus from 1988-1996. Modified from Sharafan and Markov (2001).

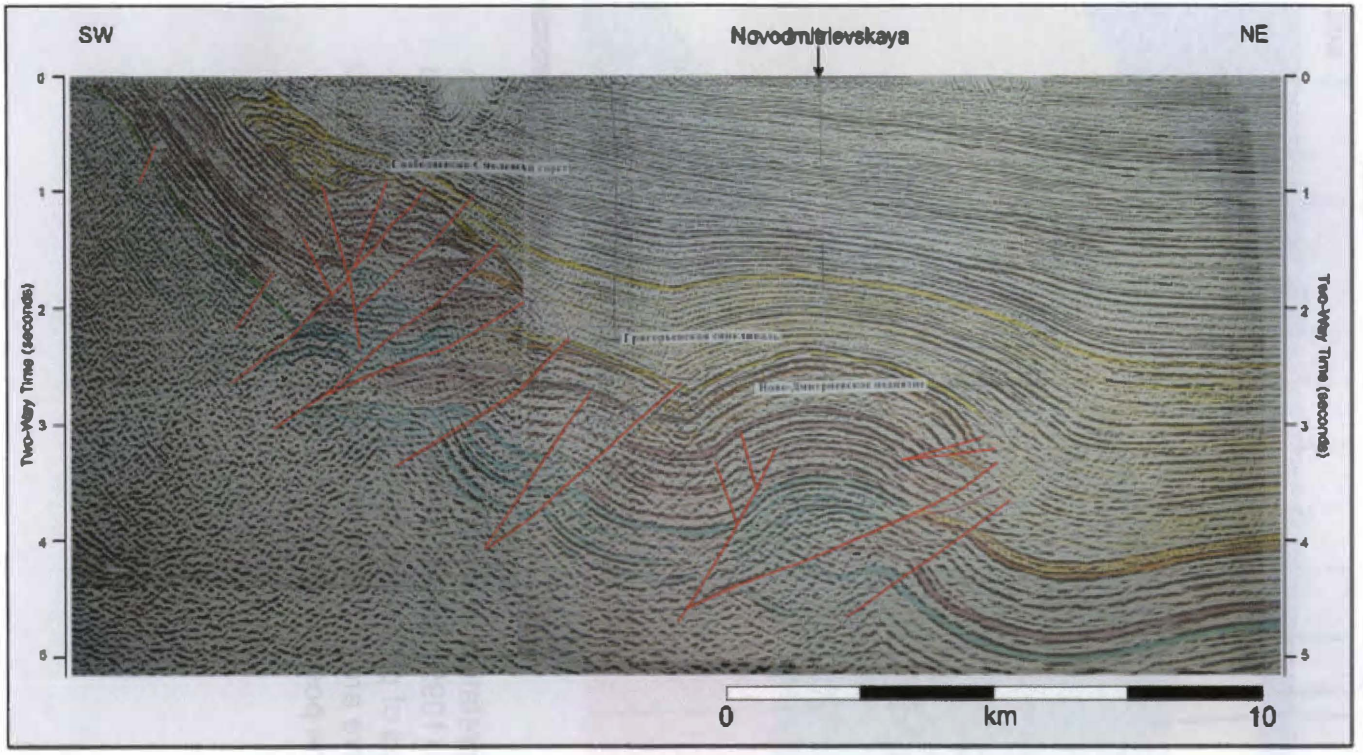

Figure 7. Soviet-era seismic time section acquired by Krasnodar Neftegeofizika in the mid-1980's. Shown is a partially interpreted (major reflectors in color, faults in red) regional-scale profile extending from the northern Caucasus foothills in the direction of the Black Sea coast to northeast of Novodmitrievskaya. Kutsenko (2002).

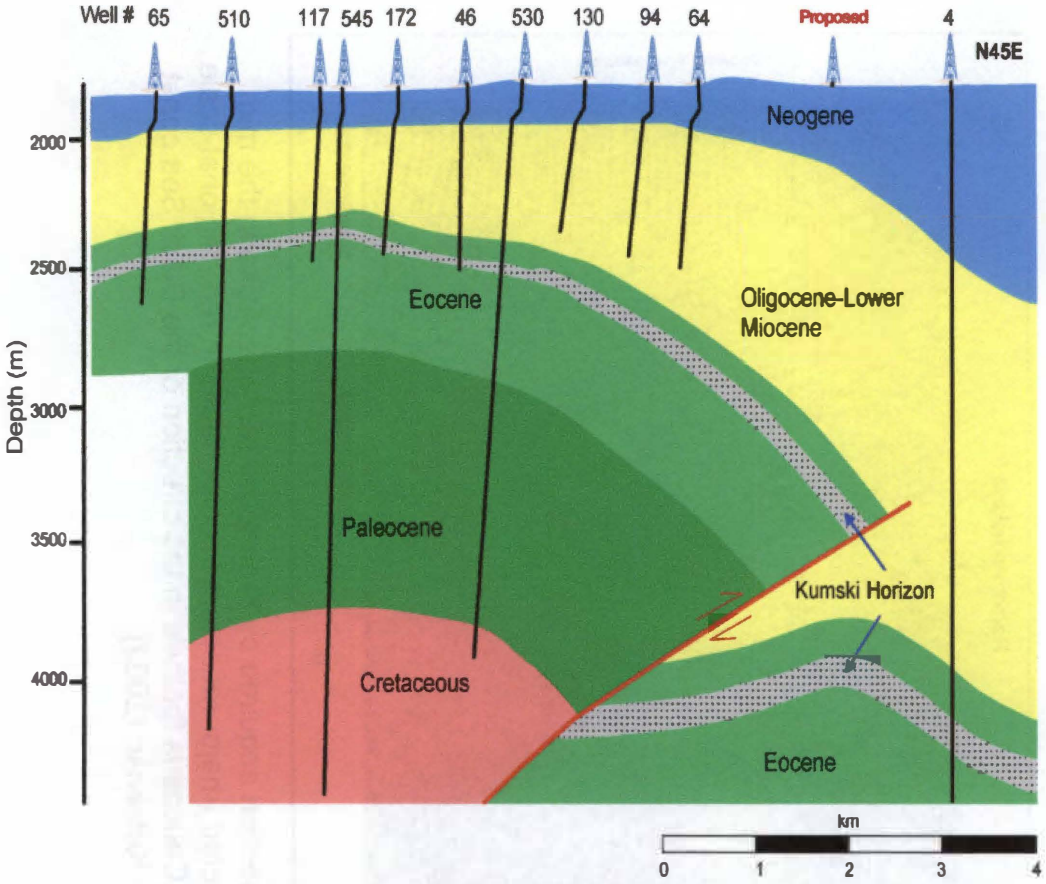

Figure 8. Interpretation of the Shebsh structure by Krepenevich and Karrilenko (1995), based on well data including Well 4, and several vintages of proprietary seismic reflection data. Critical points to observe are (1) the amount displacement on the thrust fault, and (2) the position of Well 4 relative to the structure.

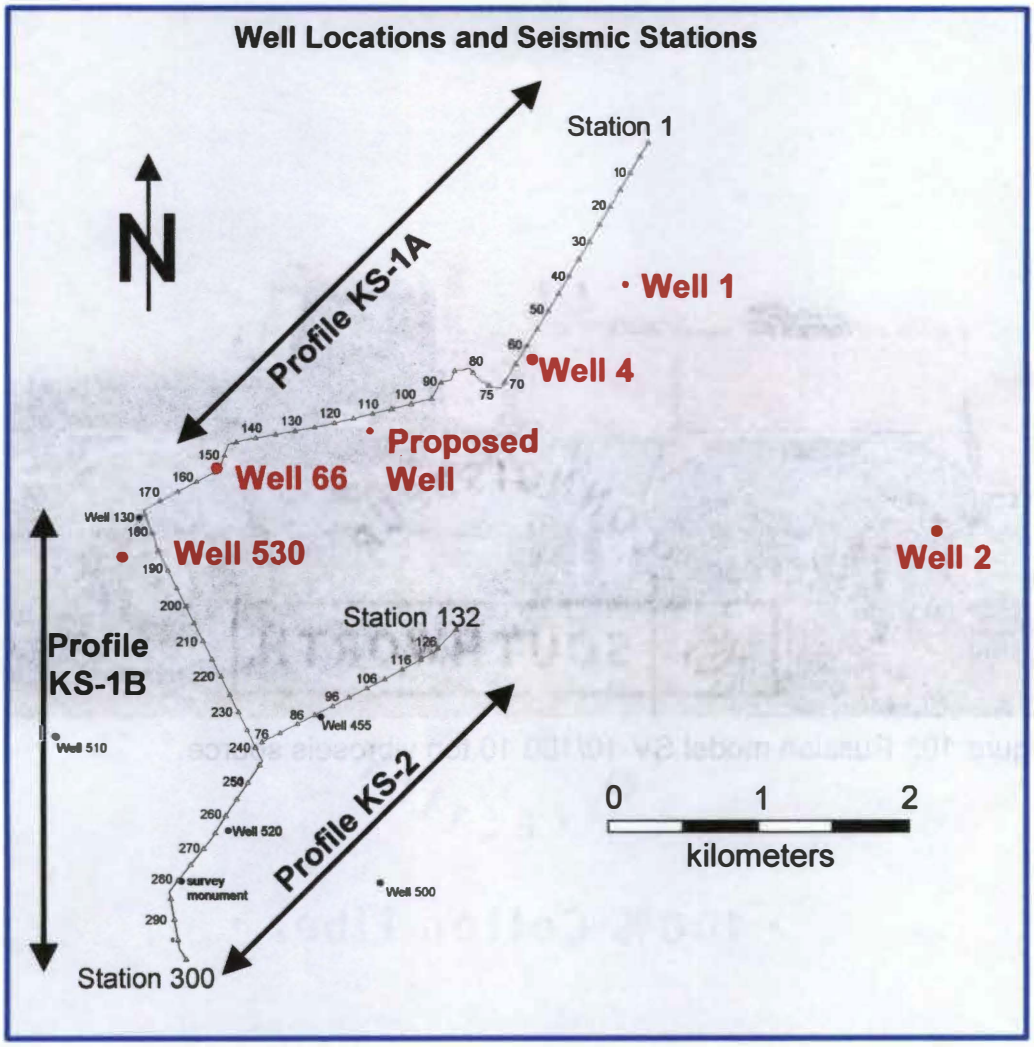

Figure 9. Location map for seismic profiles 1A, 1B, and 2 in the Shebsh field with well locations and seismic station numbers. The irregular distribution of the stations is due to the existing roads that the SV-10/180 vibrator and other vehicles could travel.

Figure 10. Russian model SV-10/180 10 ton vibroseis source.

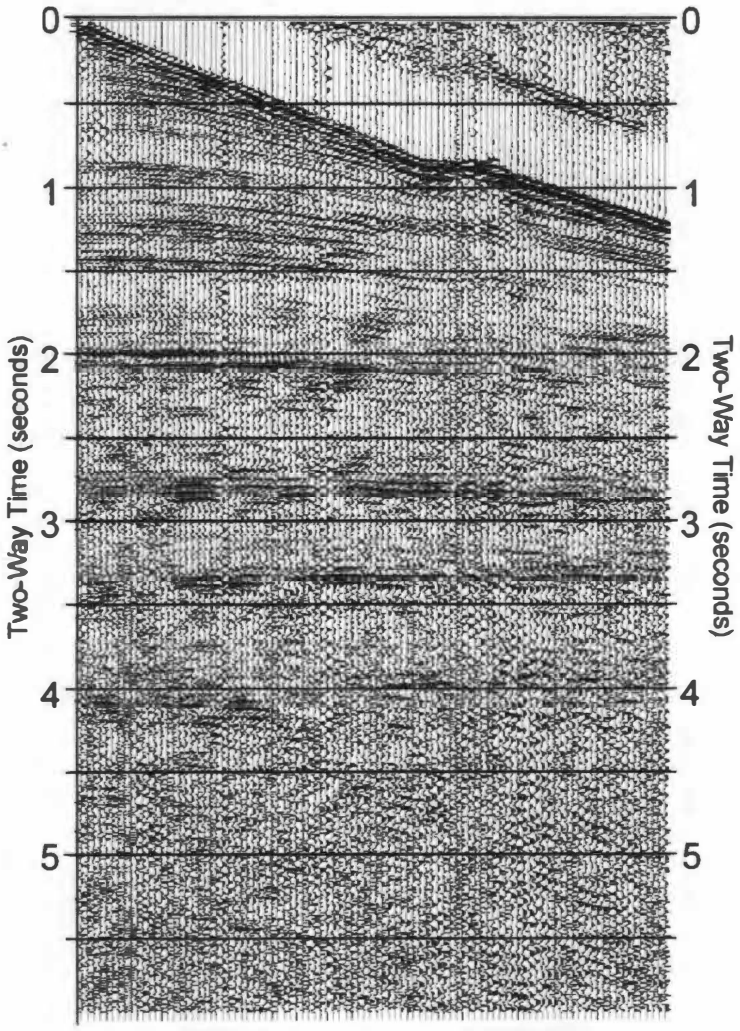

Figure 11. Example shot gather from profile 1A. Effect of the crooked line is evident in the times of the first arrivals.

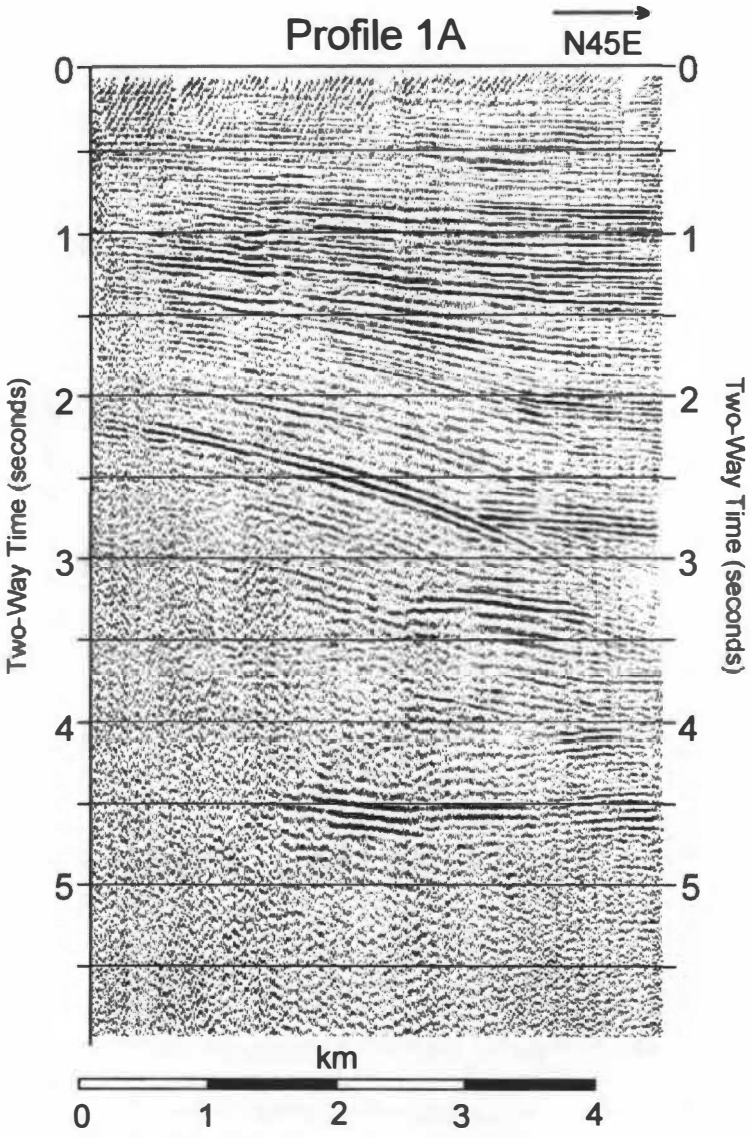

Figure 12. Unmigrated seismic time section for profile 1A.

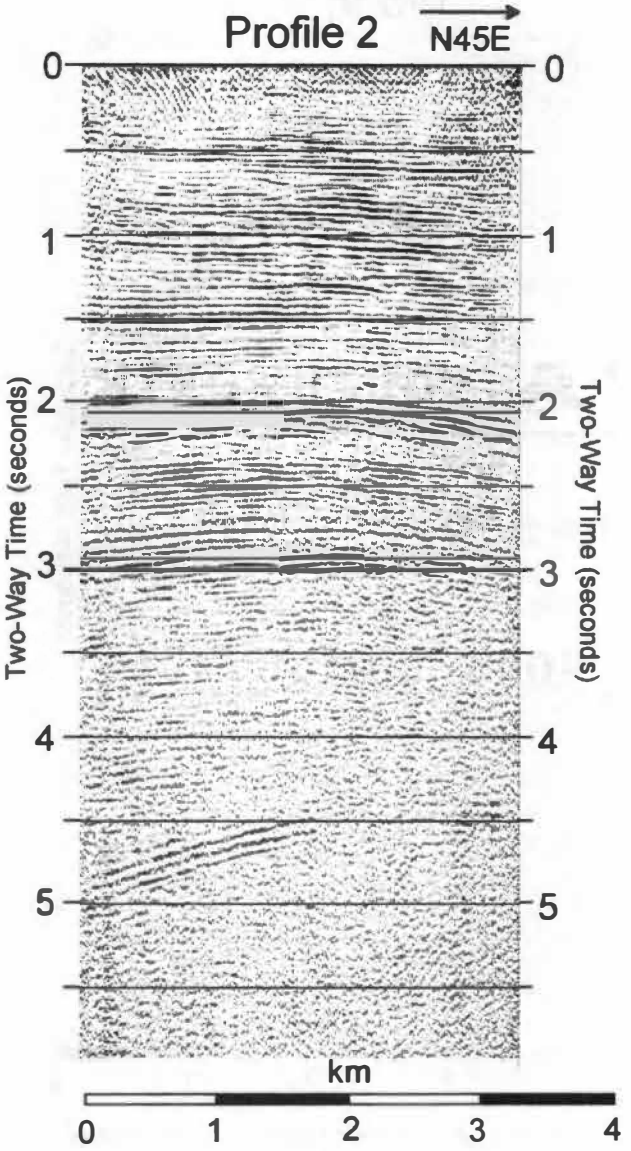

Figure 13. Unmigrated seismic time section for profile 2.

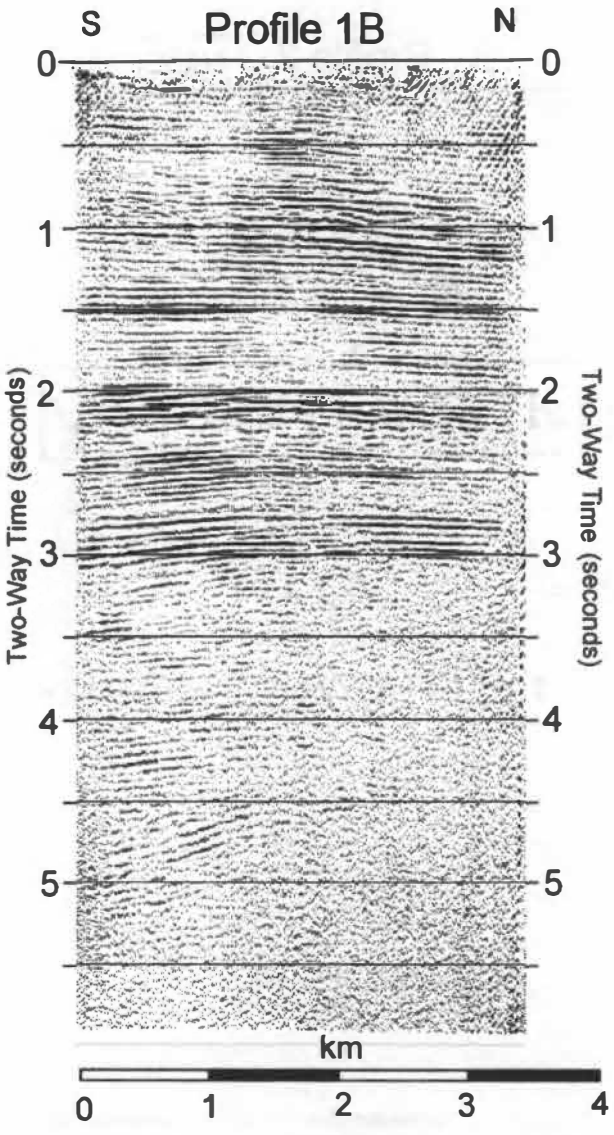

Figure 14. Unmigrated seismic time section for profile 1B.

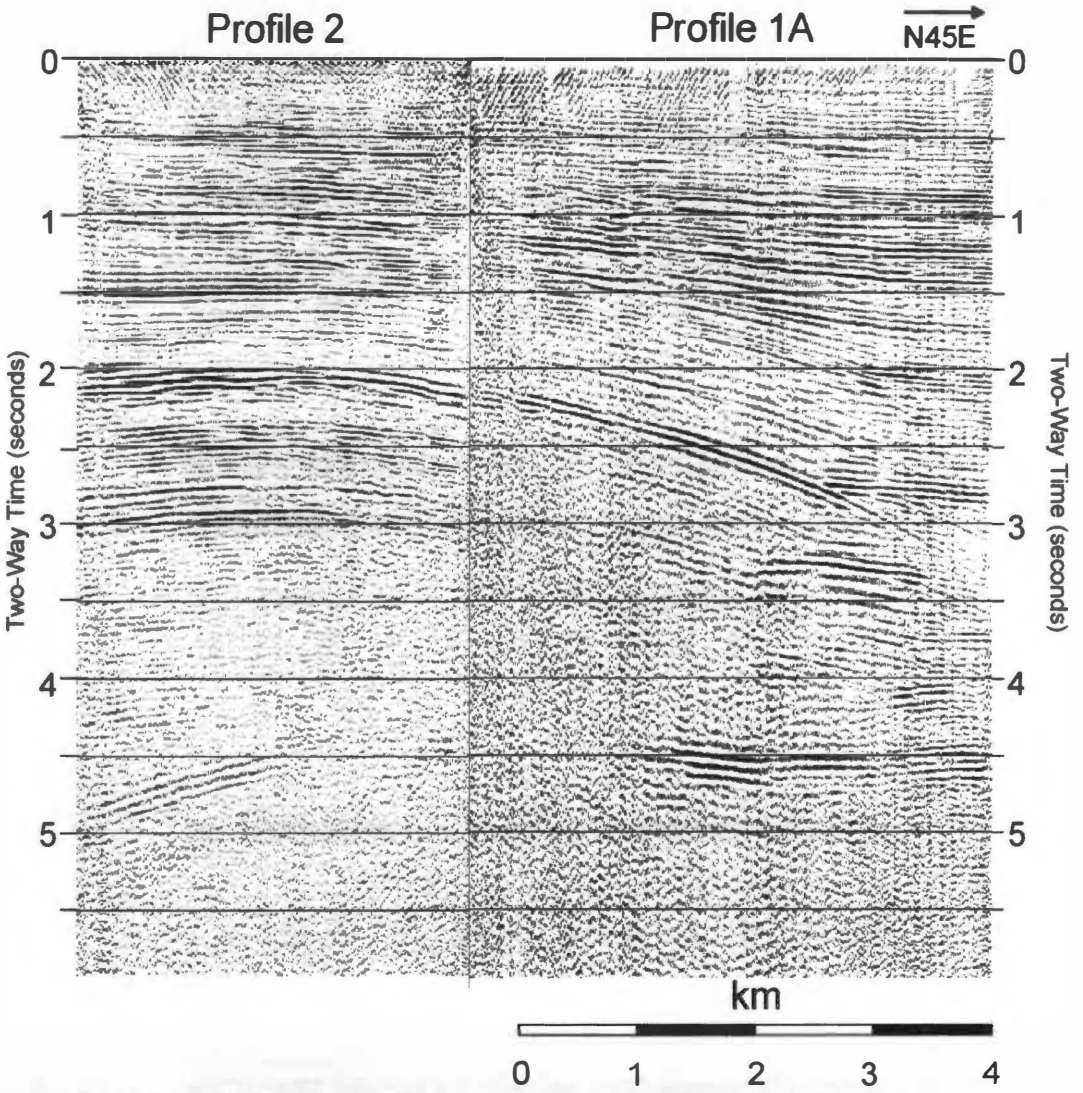

Figure 15. Profiles 1A and 2 displayed together, with the overlapping portion of 1A removed.

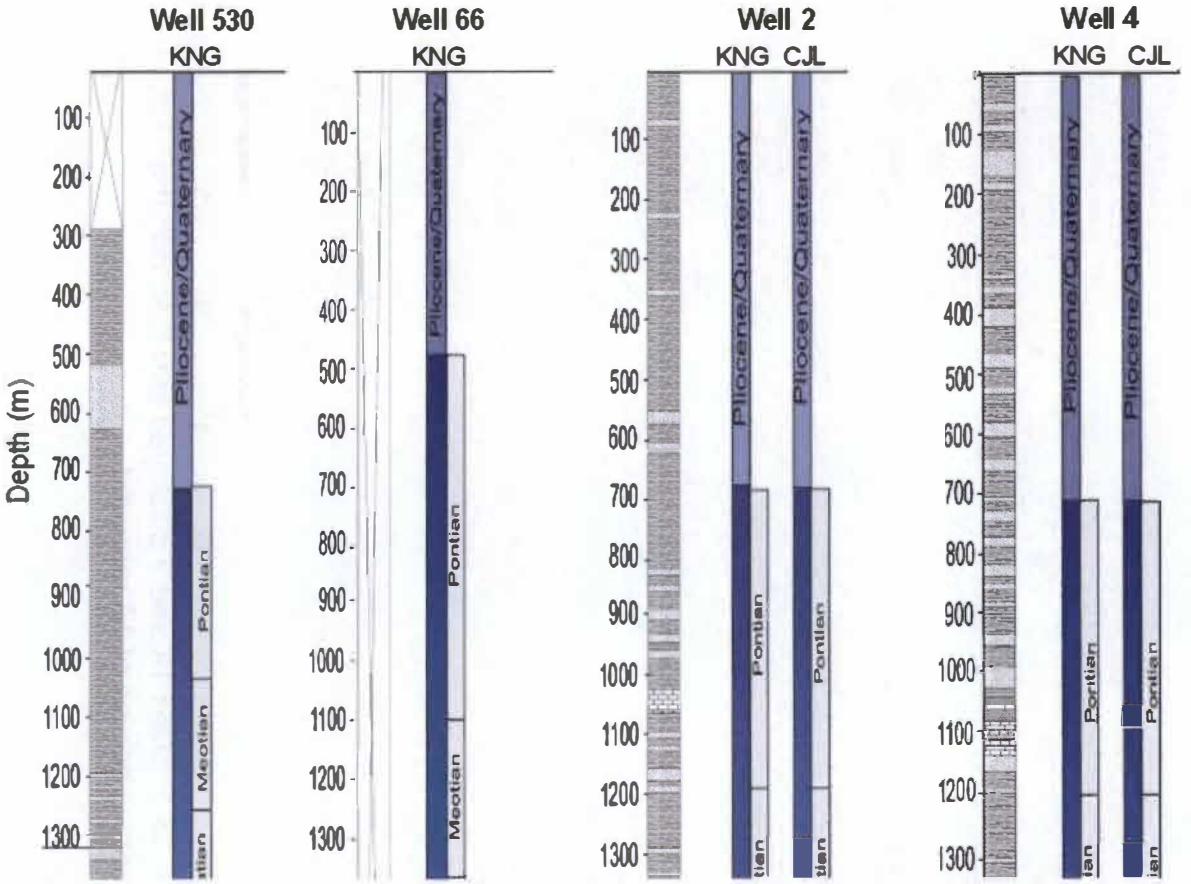

Figure 16. Wells 2, 4, 66, and 530 used in this study. KNG is the well log constructed by Krasnodar Neftegeofizika (Kutsenko, 2002). CJL is reinterpreted.

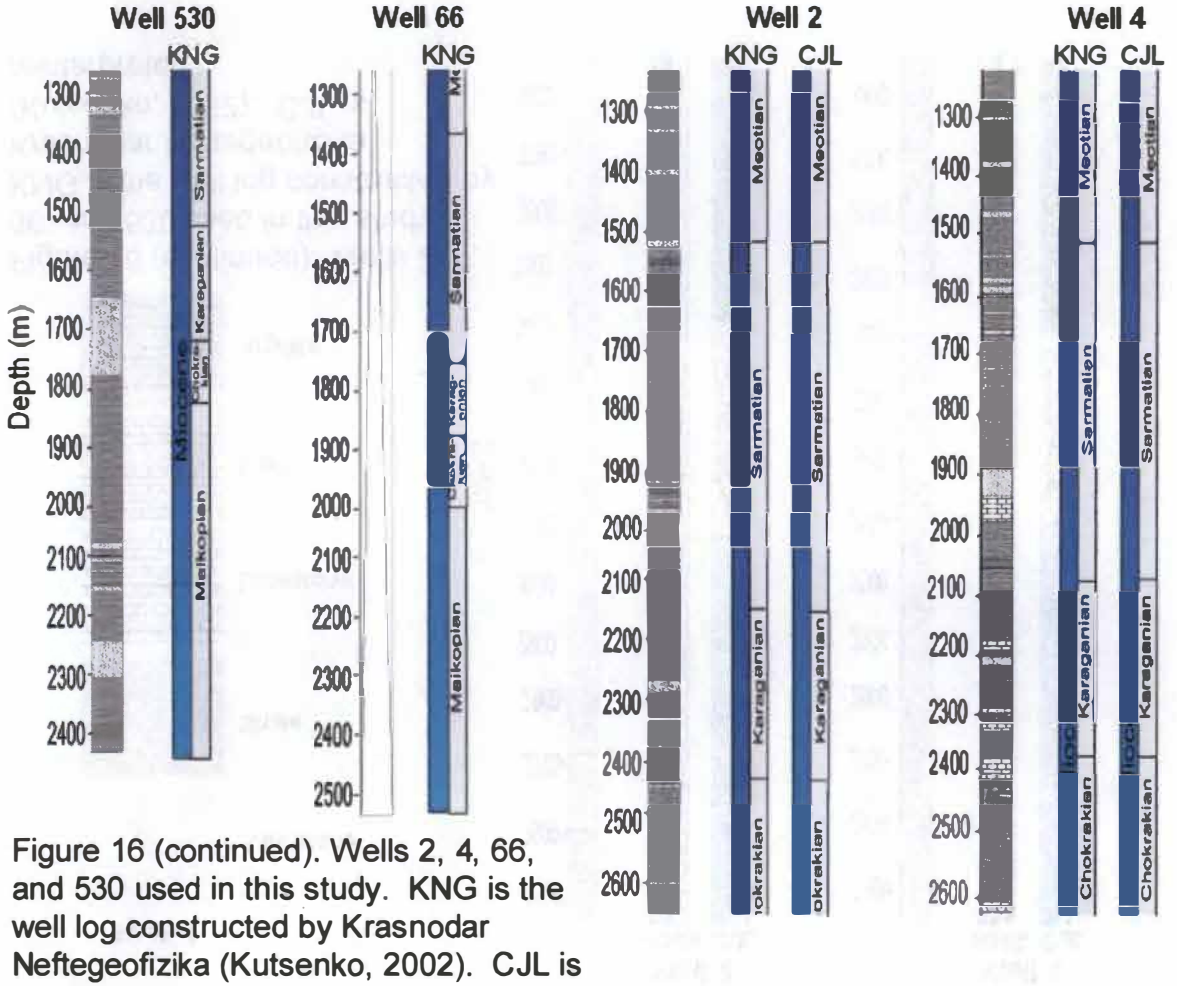

Figure 16 (continued). Wells 2, 4, 66, and 530 used in this study. KNG is the well log constructed by Krasnodar Neftegeofizika (Kutsenko, 2002). CJL is reinterpreted.

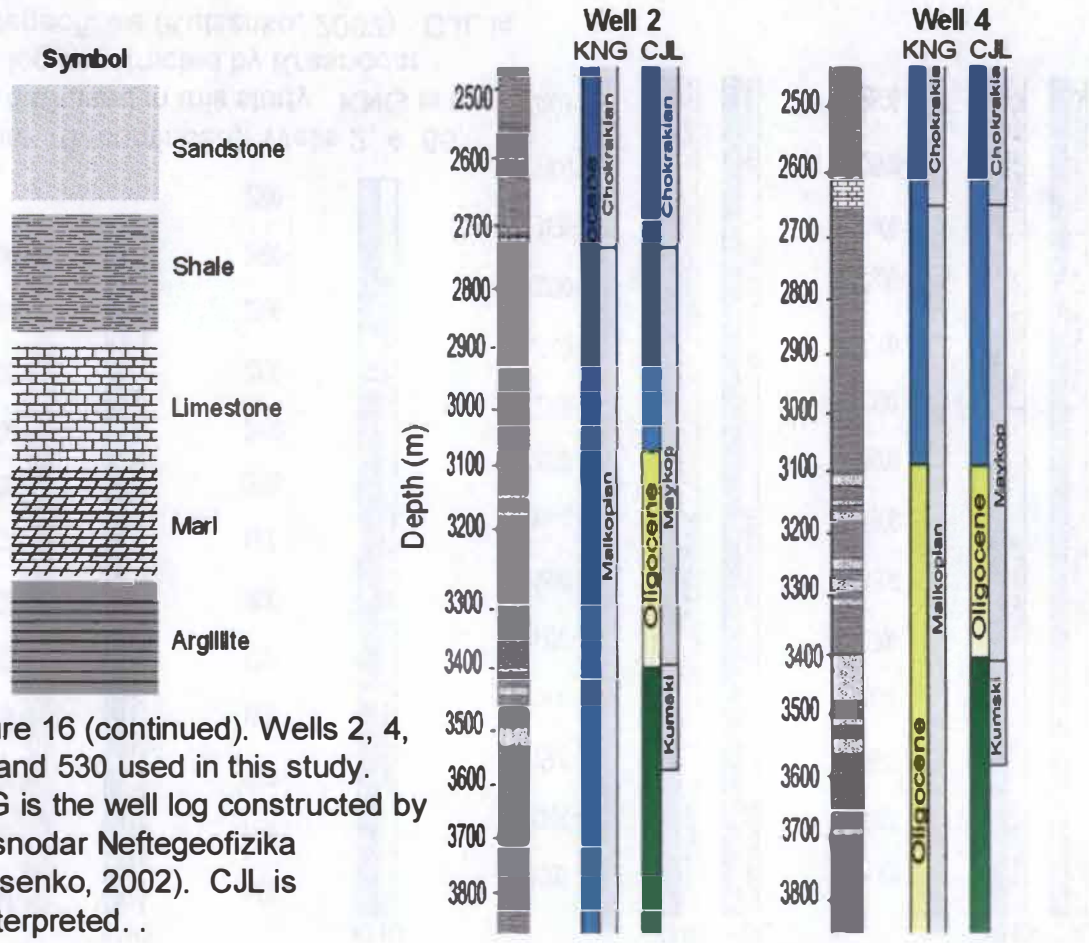

Figure 16 (continued). Wells 2, 4, 66, and 530 used in this study. KNG is the well log constructed by Krasnodar Neftegeofizika (Kutsenko, 2002). CJL is reinterpreted. .

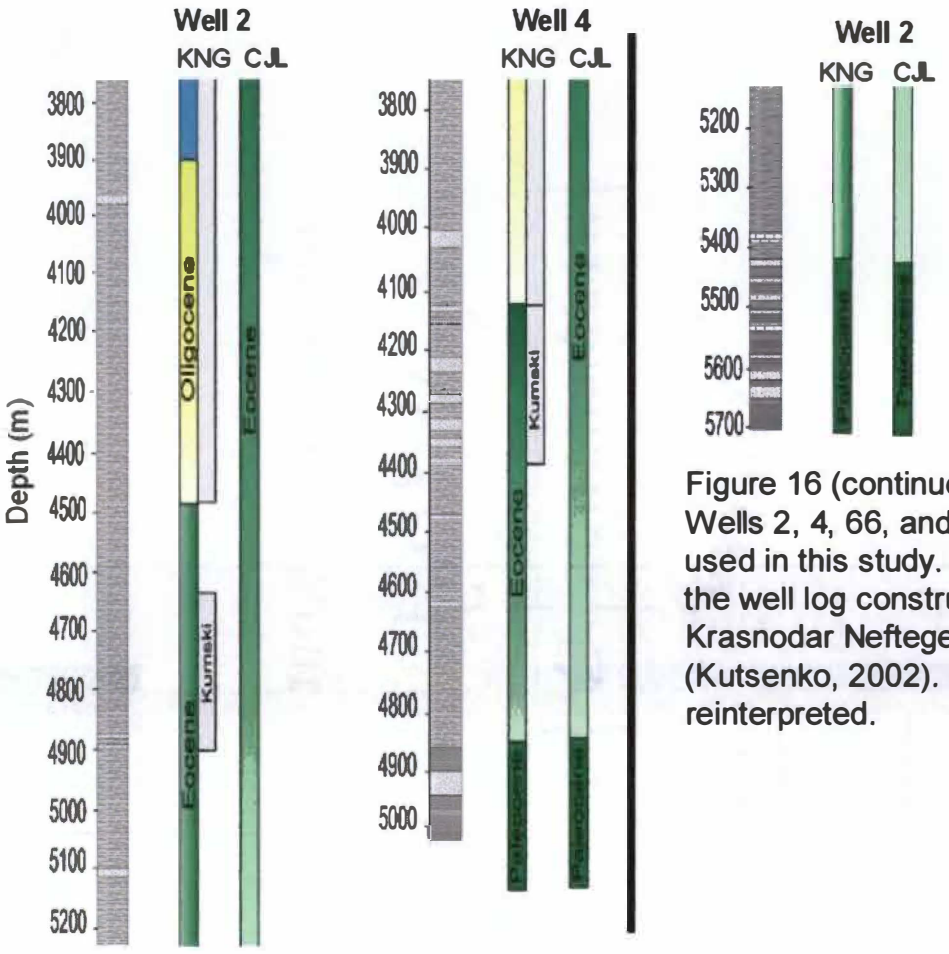

Figure 16 (continued). Wells 2, 4, 66, and 530 used in this study. KNG is the well log constructed by Krasnodar Neftegeofizika (Kutsenko, 2002). CJL is reinterpreted.

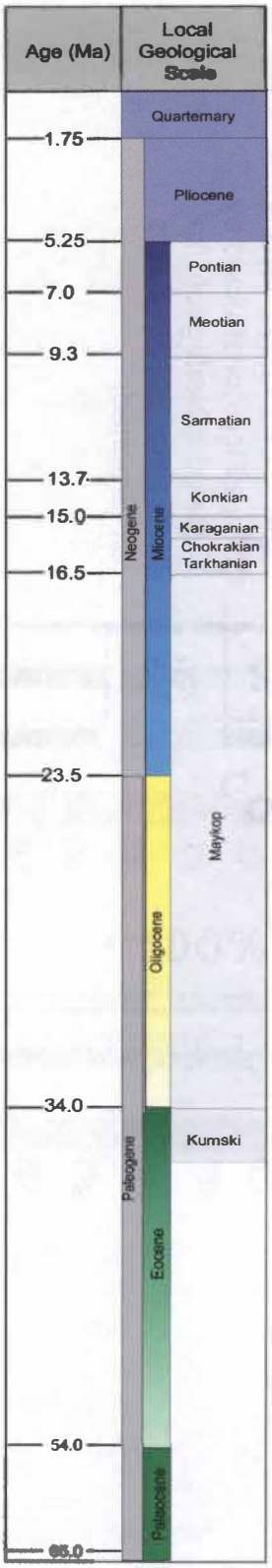

Figure 17. Local geologic time scale for the western Kuban Basin. Data from Ershov et al. (1999).

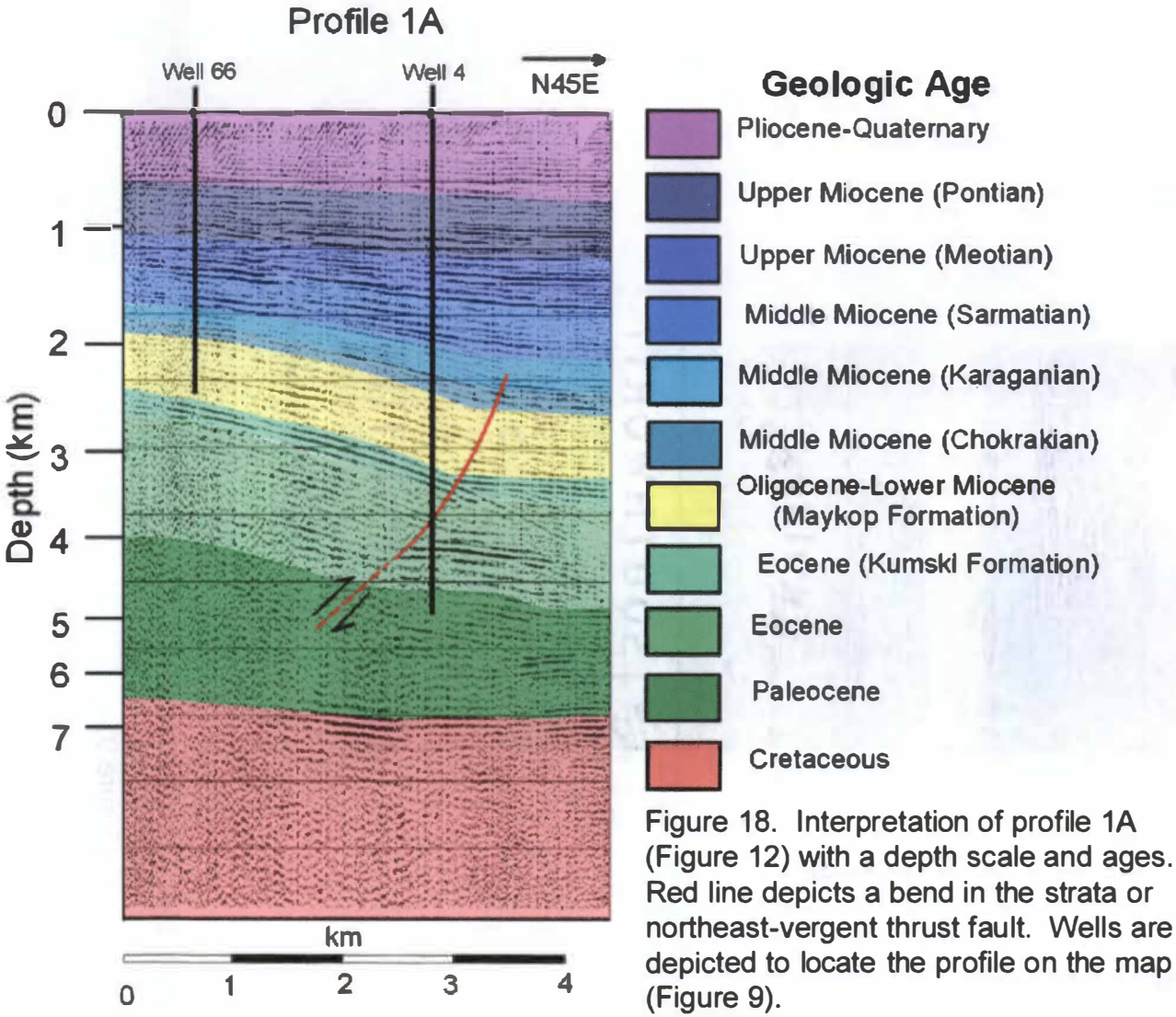

Figure 18. Interpretation of profile 1A (Figure 12) with a depth scale and ages. Red line depicts a bend in the strata or northeast-vergent thrust fault. Wells are depicted to locate the profile on the map (Figure 9).

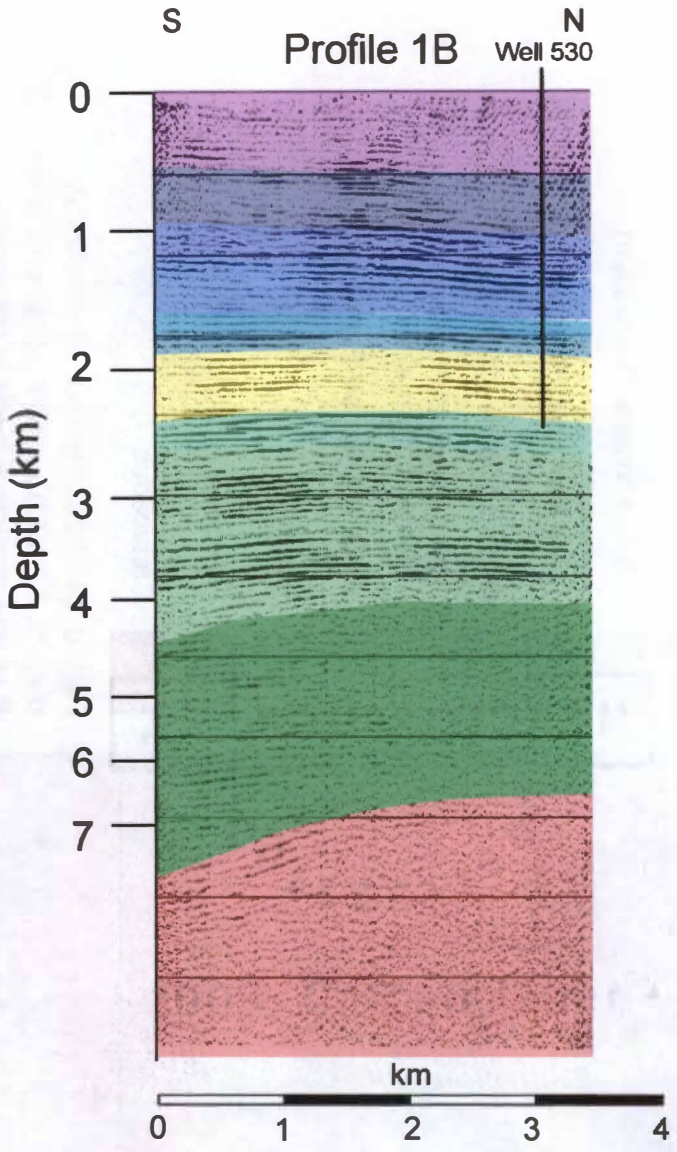

Figure 19. Interpretation of profile 1B (Figure 14) with a depth scale and ages. Well 530 is depicted to locate the profile on the map (Figure 9).

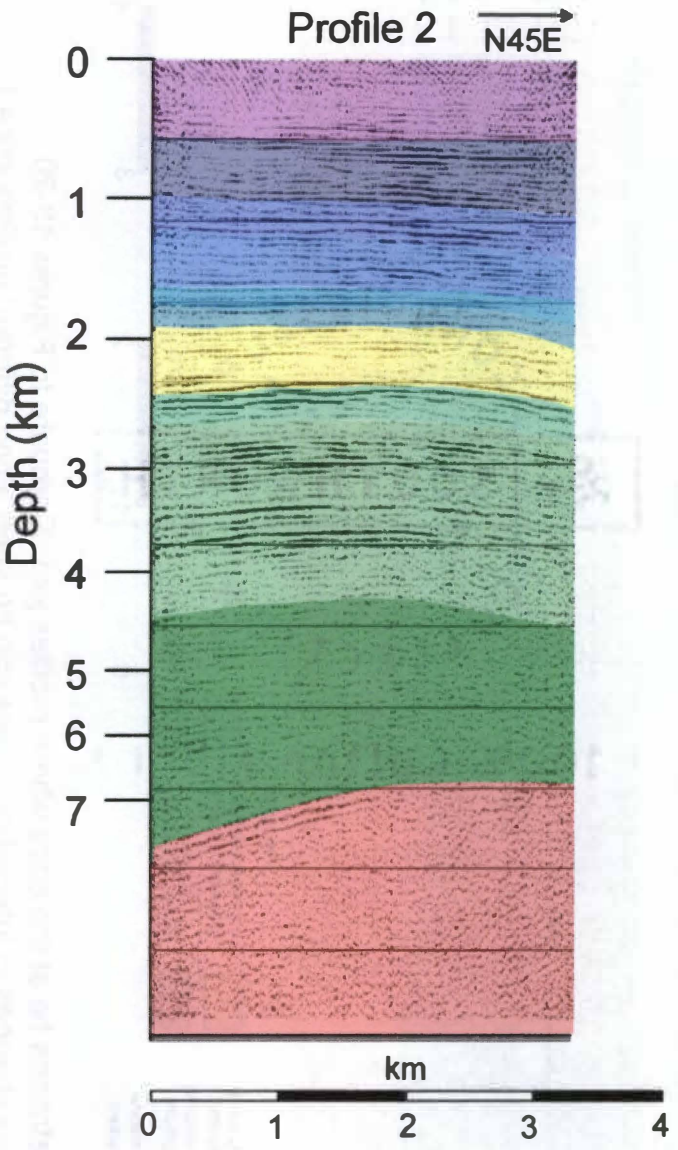

Figure 20. Interpretation of profile 2 (Figure 13) with a depth scale and ages.

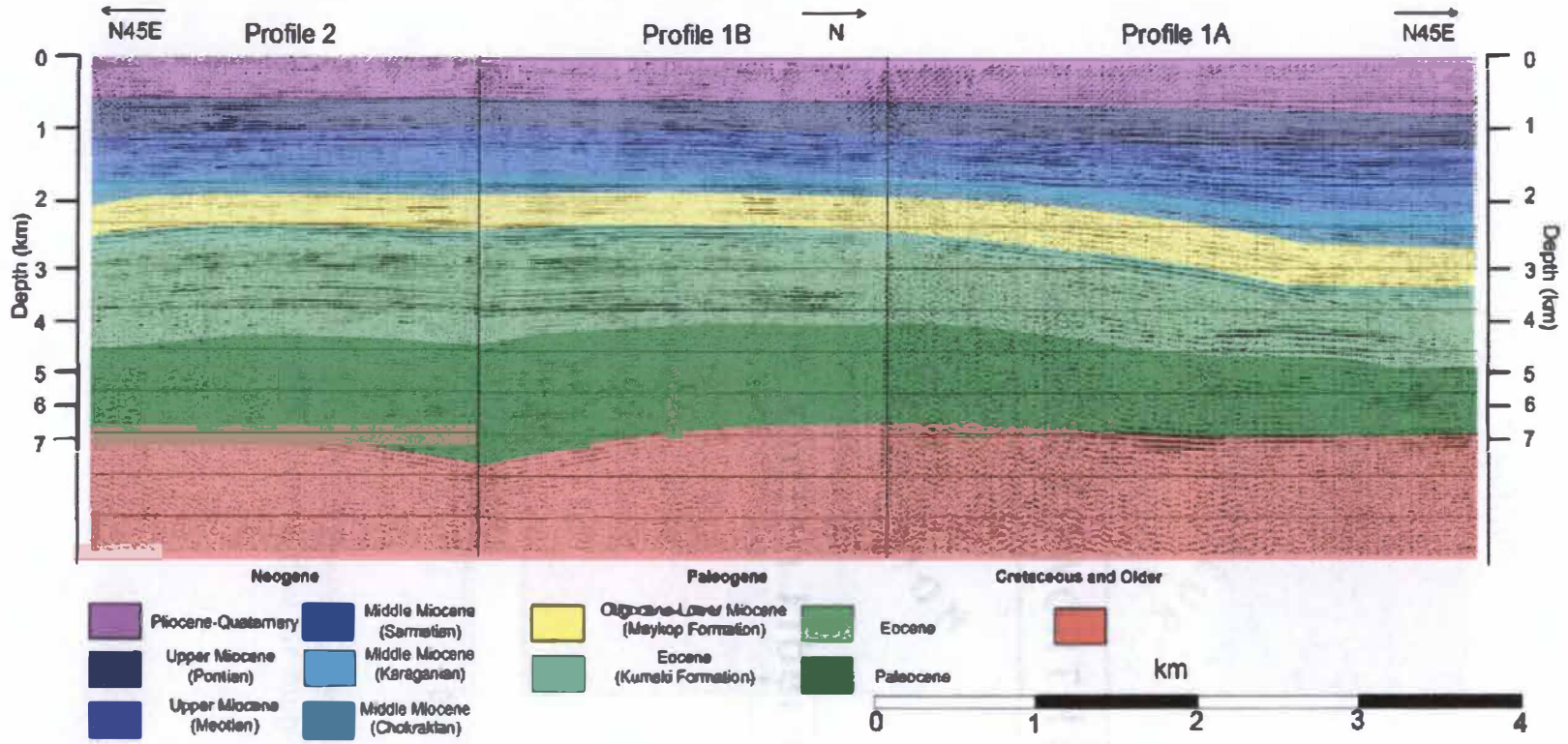

Figure 21. Seismic interpretations tie at the ends where profiles join. Compare to Figures 18-20. Significant three-dimensional changes in interval thickness can be seen along different profiles in part due to differing amounts of tectonic shortening.

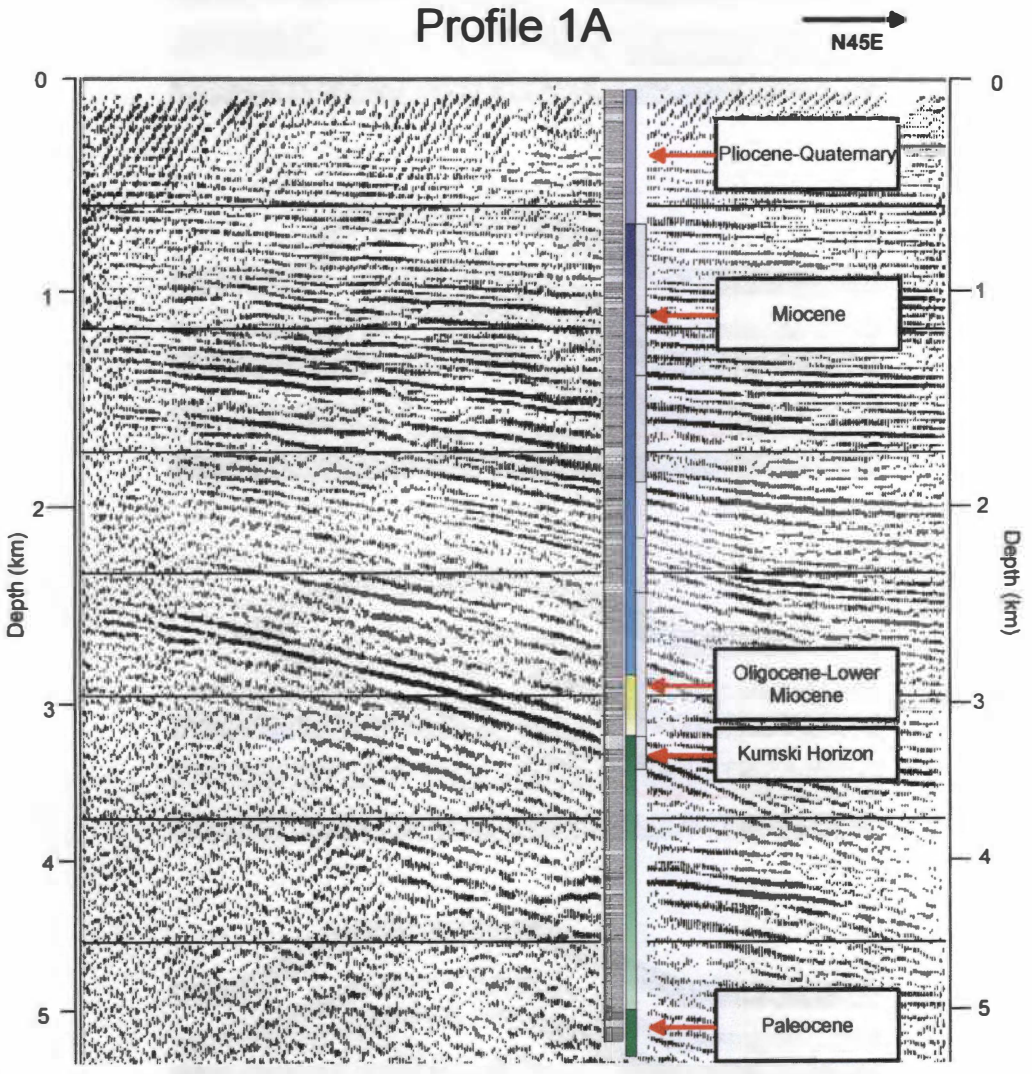

Figure 22. Well 4 compared to profile 1A. The bright reflectors at ~4.3 km depth are sand bodies, and may or may not be the Kumski horizon.

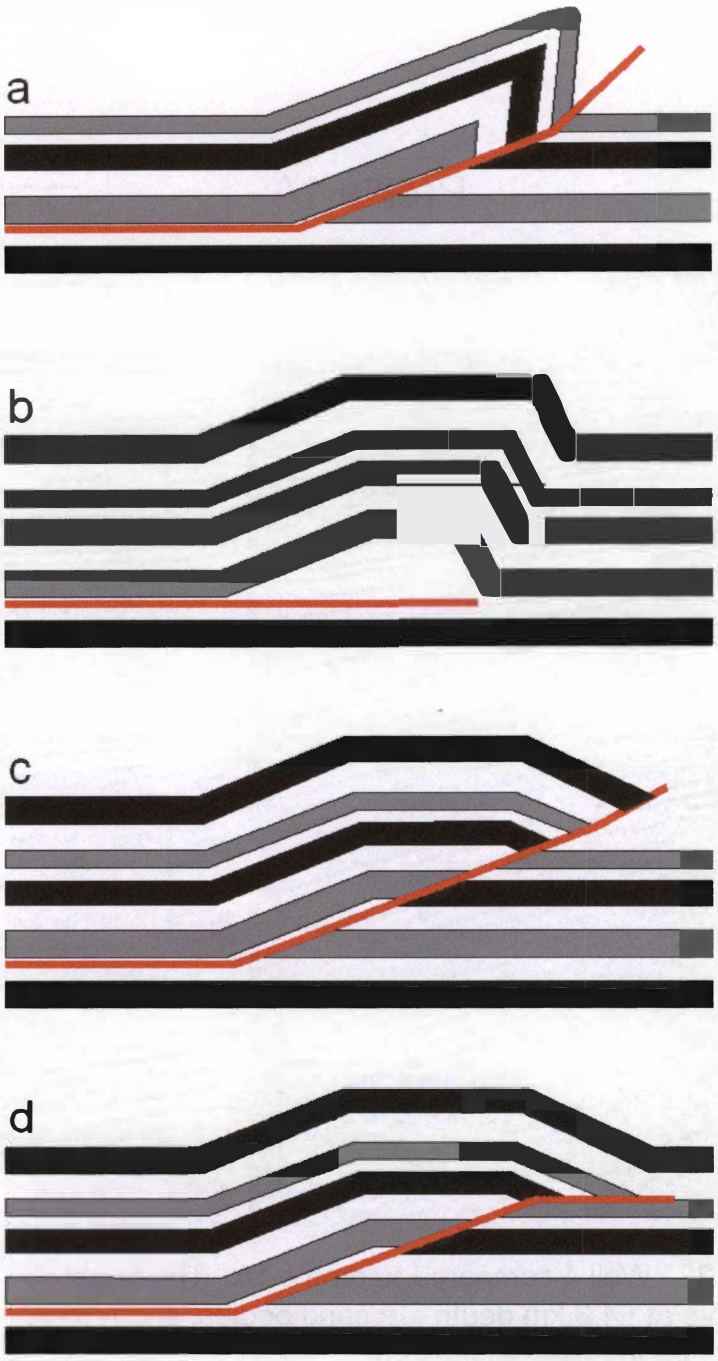

Figure 23. Schematic diagrams of the principle fault-related fold types for comparison with the anticline at the Shebsh field: a) fault-propagation fold, b) detachment fold, c) fault-arrest fold, and d) fault-bend fold. Red line shows the trajectory of the underlying thrust fault. Modified from Williams and Chapman (1983), Suppe (1985), McClay (1992), and Thorbjornsen and Dunne (1997).

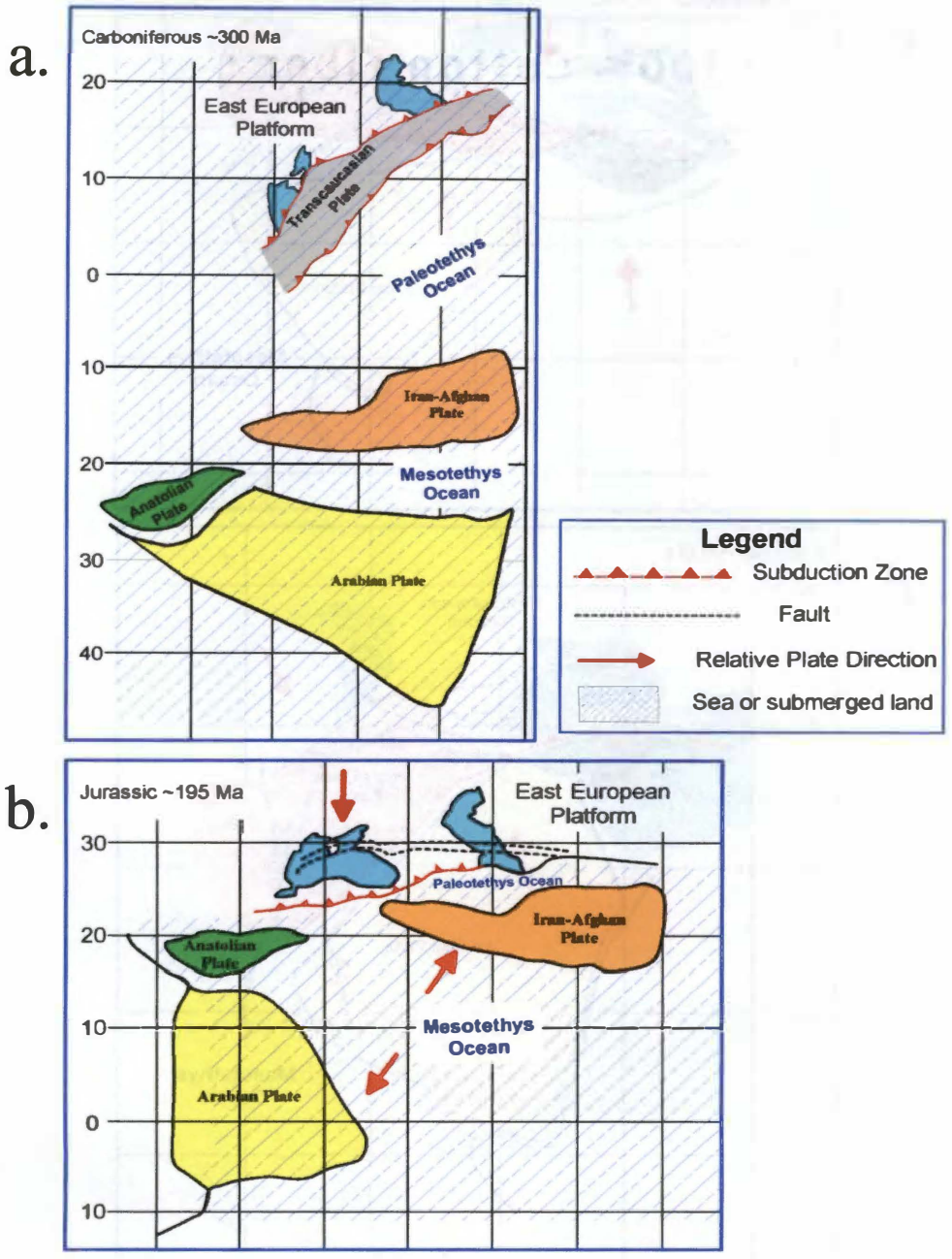

Figure 24. Tectonic plates of the Caucasus/Tehyan realm. Note that the Black and Caspian Seas are depicted only for geographic reference and did not exist until approximately the Jurassic period. Modified from Gamkrelidze (1986).

c.

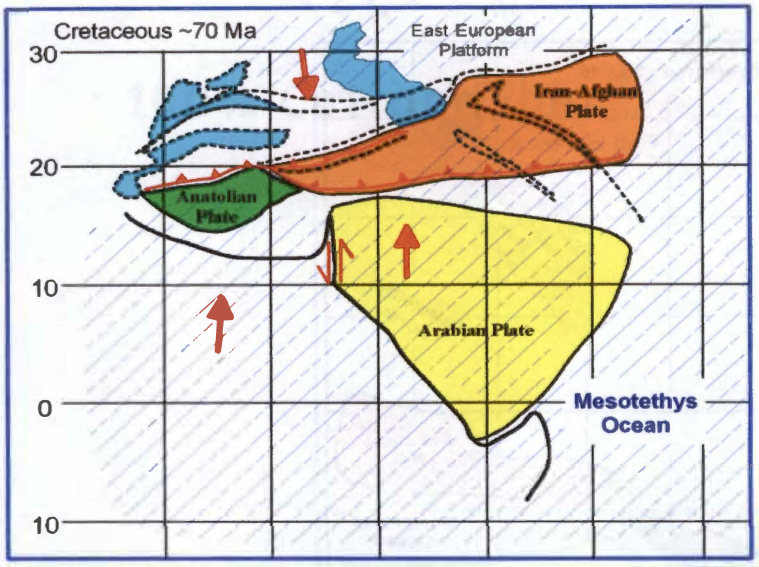

d.

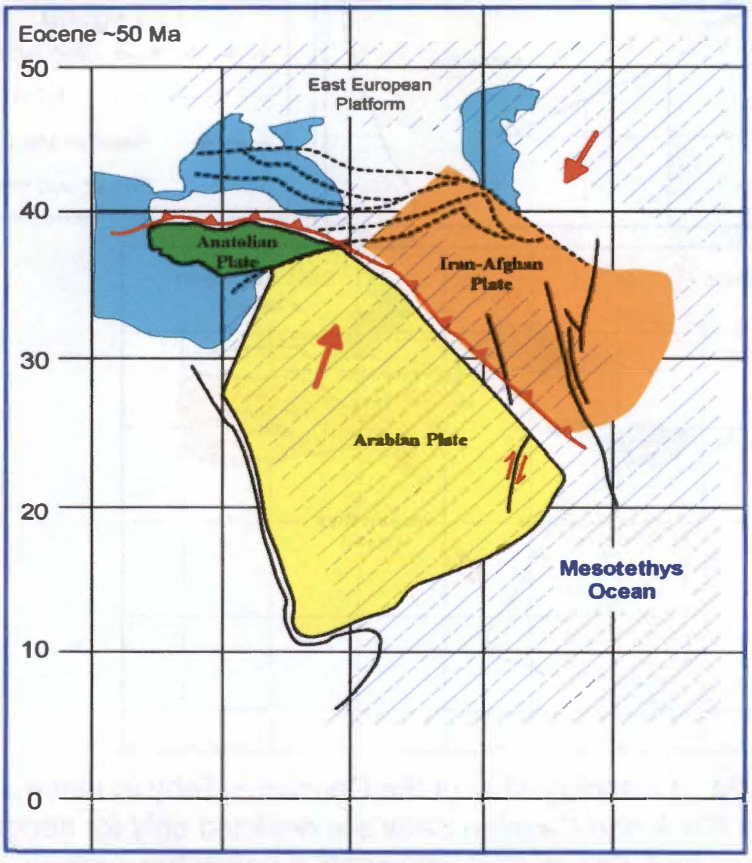

Figure 24 (continued). Interpreted plate locations of the Caucasus/Tehyan realm. Modified from Gamkrelidze (1986).

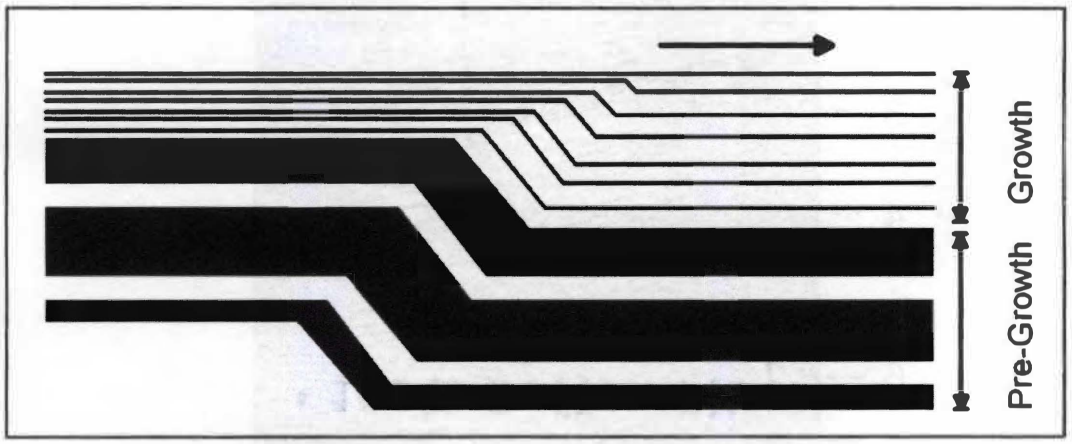

Figure 25. Model of pre-growth and growth strata for a generalized fault-related fold. Modified from Suppe et al. (1995).

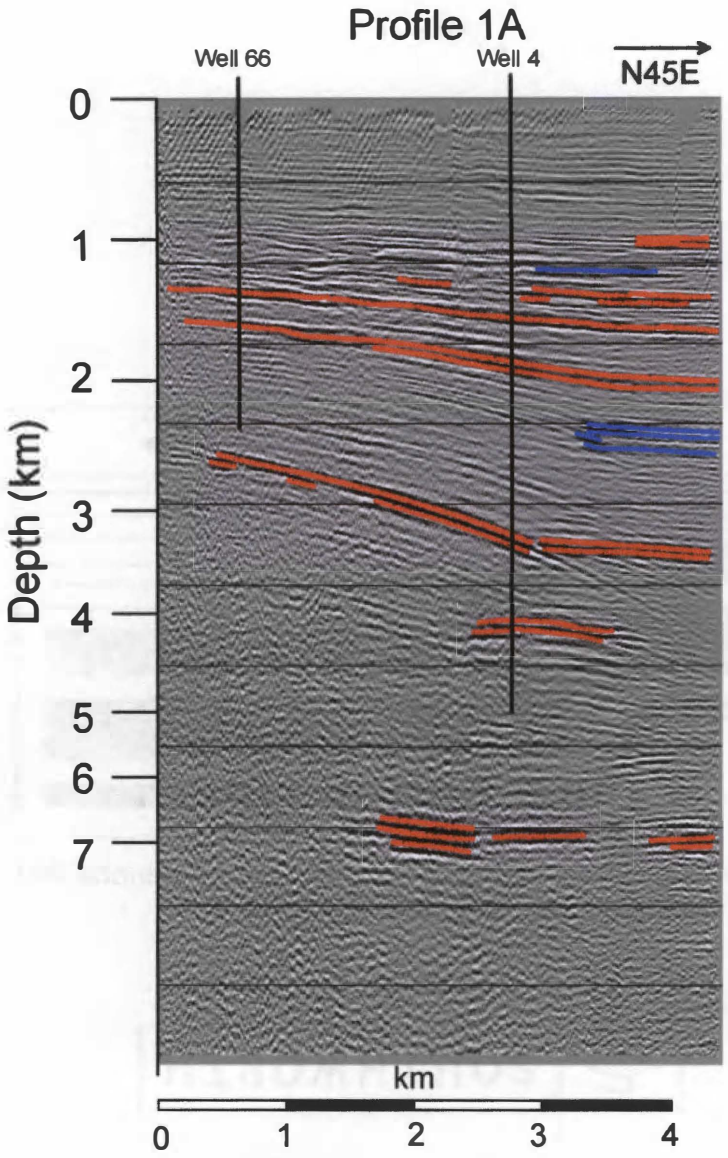

Figure 26. Locations of sandstone (red) and limestone (blue) layers that correlate with bright spots or high amplitude reflectors. a) Locations for profile 1A.

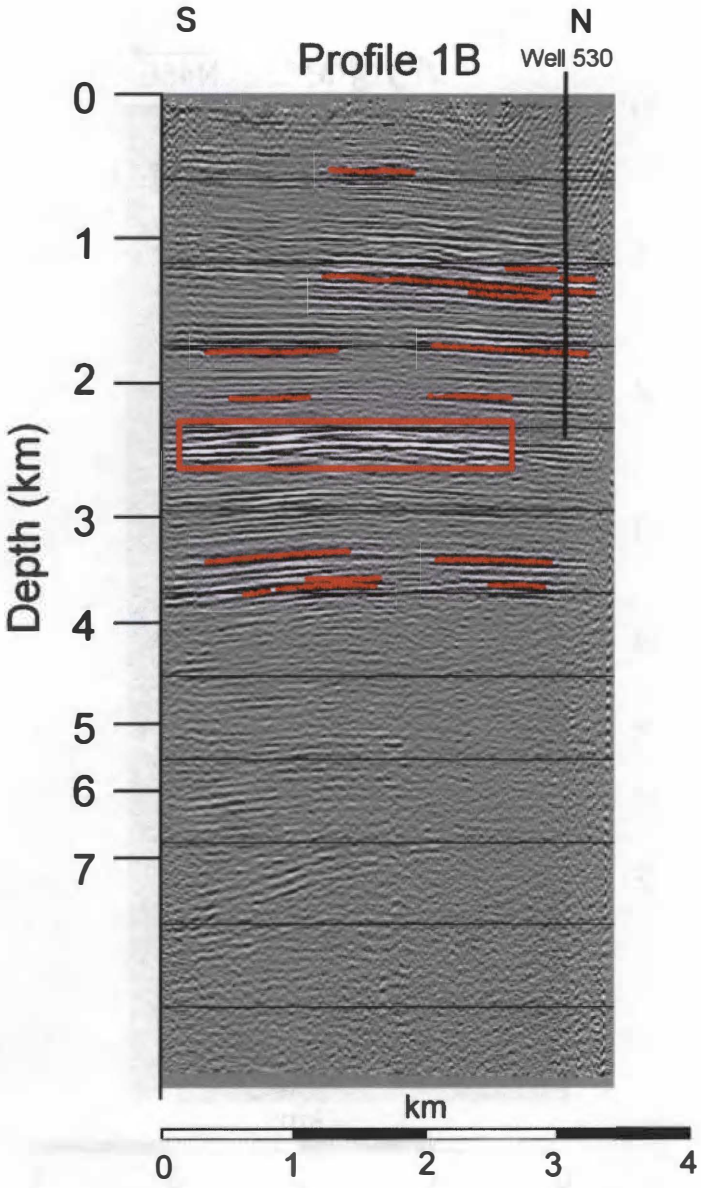

Figure 26. (continued) b) Locations for profile 1B.

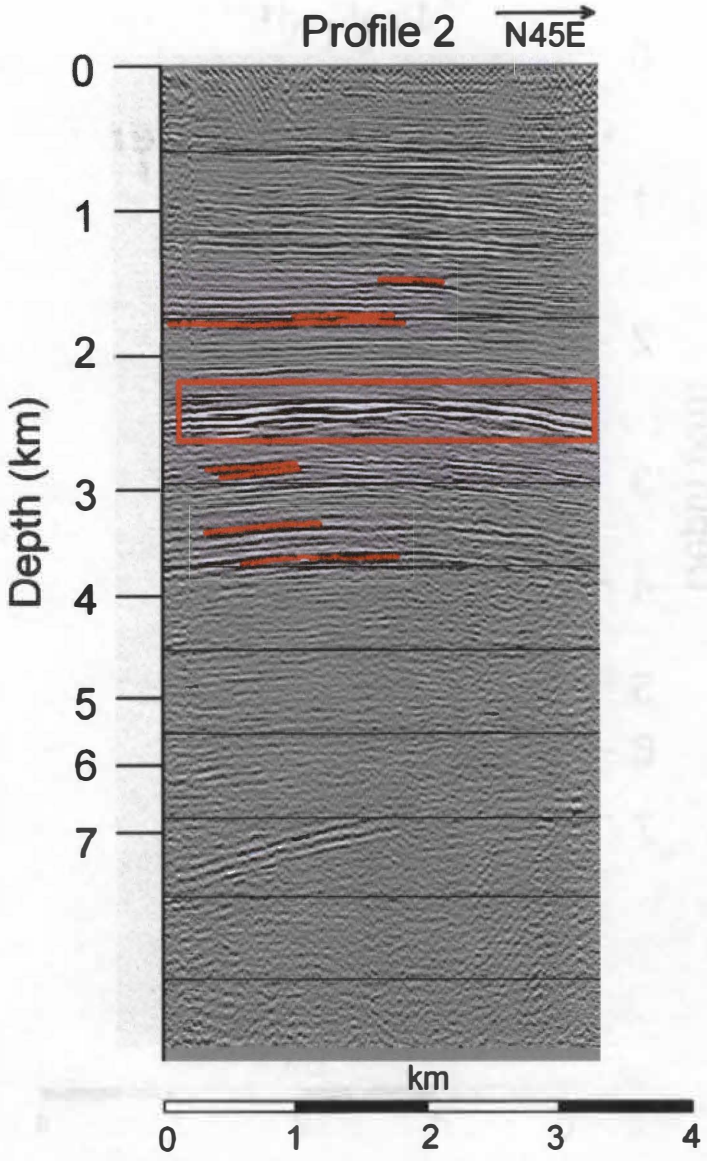

Figure 26. (continued) c) Locations for profile 2.

Vita

Charles Joel Luckow Jr. was born April 1, 1977, and raised in Metairie, Louisiana. He graduated from Archbishop Rummel High School in 1995 and attended the University of New Orleans, where he received a B.S. in Geophysics in the fall of 2000. One year later, he moved to Knoxville, Tennessee, to pursue an M.S. in Geology from the University of Tennessee. During the summer of 2002, Joel interned aboard a seismic vessel in the Gulf of Mexico with Western-Geco. The following summer, he completed an internship at ExxonMobil Exploration Company in Houston, TX, working with eastern Gulf of Mexico group. He received his M.S. in Geology in the fall of 2003. Joel is currently employed at ExxonMobil Exploration Company in Houston, Texas, and hopes to build a career as a geophysicist.